

The Analytical Theory of Bulk Melting II: Variational Method Solution in the FCC Crystal

Yajun Zhou ^{*} and Xiaofeng Jin [†]

Surface Physics Laboratory & Department of Physics, Fudan University, Shanghai 200433, China

(Dated: November 5, 2018)

Continuing the arguments in Paper I (arXiv: cond-mat/0405487), we model the temperature dependence of interstitial defects in a surface-free face-centered-cubic (fcc) elemental crystal and obtain the free energy and correlation behavior based on variational methods. We show that the avalanche of interstitial defects is the instability mechanism at the melting point that bridges Lindemann and Born criteria.

PACS numbers: 64.70.Dv, 64.60.Qb

I. INTRODUCTION

Bulk melting is a solid-liquid phase transition (SLPT) taking place in a surface-free crystal [1]. The study of this phenomenon helps to clarify the essential driving force of the inhomogeneous phase transition out of a homogeneous system in that the surface-free condition rules out the influence of inhomogeneity at the surface boundary. Many endeavors have been made to test the previous melting theories by probing into the behavior of bulk melting [2], especially in search of the relation between the widely-cited Lindemann [3] and Born [4] criteria. Lindemann criterion proposes that melting is triggered by the avalanche of the root-mean-square (rms) atom displacement after it exceeds a threshold fraction (δ_L^*) of the atom spacing (a), where δ_L^* is called the critical Lindemann ratio, a semi-empirical parameter once conceived as a lattice type characteristic; Born criterion argues that the vanishing of the shear modulus is responsible for the inability to resist lattice destruction at the melting point.

In the recent molecular dynamics simulation contributed by Jin *et al.* [5], it is demonstrated that the melting point of a surface-free Ar crystal does satisfy both Lindemann and Born criteria. In Ref. [5], the Ar crystal melts when the shear moduli see a sudden downfall (albeit not vanishing, which is consistent with the experimental observation of residual shear modulus at the melting point [6]) and the atom displacement surges towards infinity simultaneously. Jin *et al.* have attributed this coincidence to the “Lindemann particle” (atom with displacement larger than δ_L^* times the atom spacing) clusters that emerge sporadically at low temperatures but abound throughout the crystal when melting point is approached. It is found that within such clusters (“liquid nuclei”) consisting of energetic “Lindemann particles”, the shear moduli difference is nearly vanishing: $\Delta C_S = C_{44} - (C_{11} - C_{12})/2 \approx 0$. Judging the rôle of

“Lindemann particle clusters” that satisfy both the Born and Lindemann instability criteria, it is then concluded in Ref. [5] that melting is governed by the “strongly-correlated” Lindemann and Born perspectives. However, several important questions remain unanswered by numerical results:

Question 1: What kind of instability mechanism is directly responsible for the non-zero shear moduli at the melting point? Is that contradictory to Born’s original argument that melting is triggered by zero shear moduli?

Question 2: How does a heterogeneous nucleation process manage to come out from a homogeneous system? Does the *finite*-size of the liquid nucleus at the melting point violate the principle “phase transition in the thermodynamic limit”, which requires a system consisting of infinitely many atoms?

Question 3: What are the most important factors, in terms of the parameters of the interatomic forces, that affect the magnitude of the parameter δ_L^* ? How general is this δ_L^* [7]?

In this paper serving as an extension of the model in Paper I to the three-dimensional (3D) face-centered-cubic (fcc) elemental crystal, we report the detailed analytical procedure that joins the Lindemann and Born criteria together in the SLPT and the mathematical arguments that address the three numbered questions above. We show that the spatial correlation between interstitial defects is the impetus that triggers and propagates instability in a crystal and that eventually undermines long-range order in the surface-free solid. Following the idea of defect-motivated transition in previous literature [8, 9, 10, 11] and the previous understandings of defects’ cooperation and aggregation [9, 12, 13, 14, 15, 16, 17, 18, 19], we use the J_1 - J_2 lattice model plus vibrational Hamiltonian [20] to formulate the cooperative creation and the spatial correlation of interstitials. Our results, which are based on fewer empirical parameters than that in Ref. [11], not only epitomize the origin of instability and atom-scale pathway in the melting process with mathematical rigor but also help to elucidate the origin of “Lindemann particle clusters” and to explain the experimental fact [7] that δ_L^* is modulated by both lattice geometry and the profile of interactions.

Paper II is organized as follows: Sect. II is a brief ac-

^{*}Present address: Department of Chemistry and Chemical Biology, Harvard University, Cambridge, MA 02138, USA.

[†]To whom correspondence should be addressed. Email: xfjin@fudan.ac.cn

count of the methodology of our model for interstitial defects with a discussion of the symmetry of the Hamiltonian; Sect. III uses variational method to work out a mean field approximation (MFA) solution to the three-dimensional (3D) model, where the temperature dependence of the concentration and the correlation of interstitial defects are investigated; Sect. IV discusses the physical implications of the model solutions where analytical results are compared to data from experiments and simulation; Sect. V summarizes the results in Paper II. Appendix A provides an alternative derivation of the formula which describes the temperature dependence of concentration of defect; Appendix B gives the mathematical details involved in the evaluation of the correlation of defects.

II. MODEL HAMILTONIAN AND ITS QUALITATIVE PROPERTIES

A. Total Hamiltonian

We begin our argument with the Hamiltonian describing a system of $N = 4\ell^3$ atoms, labeled as $\alpha = 1, \dots, N$:

$$\begin{aligned} \mathcal{H} &= \sum_{\alpha=1}^N T_{\alpha} + \frac{1}{2} \sum_{\alpha=1}^N \sum_{\beta=1}^N V_{\alpha\beta} \\ &= \sum_{\alpha=1}^N T_{\alpha} + \frac{1}{2} \sum_{\alpha=1}^N \sum_{\beta=1}^N (V_{\alpha\beta}^{\text{vib}} + V_{\alpha\beta}^{\text{conf}}) \\ &= \underbrace{\sum_{\alpha=1}^N \left(T_{\alpha} + \frac{1}{2} \sum_{\beta=1}^N V_{\alpha\beta}^{\text{vib}} \right)}_{\mathcal{H}^{\text{vib}}} + \underbrace{\frac{1}{2} \sum_{\alpha=1}^N \sum_{\beta=1}^N V_{\alpha\beta}^{\text{conf}}}_{\mathcal{H}^{\text{conf}}} \quad (1) \end{aligned}$$

This Hamiltonian incorporates the kinetic energy of each atom labeled α (T_{α}) and pairwise potential energy between atoms α and β ($V_{\alpha\beta}$), where $V_{\alpha\alpha} = 0$, for $\alpha = 1, \dots, N$. For each atom labeled α , the potential energy which it experiences is the summation of the contribution from all the other atoms, which reads $\sum_{\beta=1}^N V_{\alpha\beta}$. From this sum, we extract a “vibrational potential” $\sum_{\beta=1}^N V_{\alpha\beta}^{\text{vib}}$, which is harmonically oscillating with respect to interatomic distance when the atom α is *perturbed*. The “configurational potential” $\sum_{\beta=1}^N V_{\alpha\beta}^{\text{conf}}$ is formally defined as $\sum_{\beta=1}^N (V_{\alpha\beta} - V_{\alpha\beta}^{\text{vib}})$. This Hamiltonian separation method has been employed to study the lattice vibration’s influence on the concentration of crystal defects [20].

The model in Paper II basically treats an elemental crystal with fcc structure (Ar, for instance). In order to take the interstitial defects into account, we use a lattice model with the standard NaCl-type structure. At absolute zero, the Na-like lattice is totally occupied by Ar atoms, while the Cl-like lattice is vacant and forms

the totality of octahedral holes in a perfect fcc crystal. Mathematically speaking, if one denotes a lattice position \mathbf{r} by a triad (hkl) , the Na-like (or Cl-like) lattice is characterized by odd (or even) $h + k + l$ indices. At any finite temperatures, by disregarding the vibrations and lattice distortions (that is, by neglecting the atoms’ kinetic energy and its consequences) momentarily [22], one may caricature the motion of the atoms in the solid as the stochastic hops on the two interpenetrating fcc lattices. The configurations of the system are thus exhausted by all the possible ways to arrange N atoms of a fcc elemental crystal at $2N$ possible sites, so the summation over atom-pairs could be converted to a summation over site-pairs, as long as the site occupancy rate n at position $\mathbf{r} = (hkl)$ is included in the following way:

$$\begin{aligned} \frac{1}{2} \sum_{\alpha=1}^N \sum_{\beta=1}^N V_{\alpha\beta}^{\text{conf}} &= \frac{1}{2} \sum_{\mathbf{r}} \sum_{\mathbf{r}'} J_{\mathbf{r}\mathbf{r}'}^{\text{conf}} n_{\mathbf{r}} n_{\mathbf{r}'} \\ &\approx \frac{1}{2} \sum_{h,k,l=1}^{2\ell} n_{hkl} \left(J_1 \sum_{|h-h'|+|k-k'|+|l-l'|=1} n_{h'k'l'} \right. \\ &\quad \left. + J_2 \sum_{|h-h''|+|k-k''|+|l-l''|=2} n_{h''k''l''} \right) \quad (2) \end{aligned}$$

Here, $\sum_{\mathbf{r}}$ denotes summation over all the $2N$ sites, and $n_{\mathbf{r}}$ denotes the number of the atoms occupying the site at position \mathbf{r} , and $n_{\mathbf{r}} = 0$ or 1. The “coupling constant” $J_{\mathbf{r}\mathbf{r}'}^{\text{conf}}$ in Eqn. (2) equals to $V_{\alpha\beta}^{\text{conf}}$ when the distance between two atoms α and β is $|\mathbf{r} - \mathbf{r}'|$. We have used the following cutoff in Eqn. (2): $J_{\mathbf{r}\mathbf{r}'}^{\text{conf}} = J_1$ when $|\mathbf{r} - \mathbf{r}'|$ = the nearest-neighbor (NN) distance, namely, the distance between a pair of nearest “Na” and “Cl”; $J_{\mathbf{r}\mathbf{r}'}^{\text{conf}} = J_2 < 0$ when $|\mathbf{r} - \mathbf{r}'|$ = the next-nearest-neighbor (NNN) distance, namely, the distance between a pair of nearest “Na” sites (or “Cl” sites); $J_{\mathbf{r}\mathbf{r}'}^{\text{conf}} = 0$ otherwise. In order that the NNN distance becomes the bond length in the fcc crystal in our model (such as Ar, as opposed to NaCl), we require that $J_1 > J_2$ and $J_2 < 0$. This J_1 - J_2 lattice model approximation is justified for interatomic forces that are both pairwise and short-ranged, which is physically applicable to solids where the interaction is governed by the Lennard-Jones (as in noble gases) or Morse functions (as in some metals) [19].

Therefore, in the fcc crystal with $2N = 8\ell^3$ sites and $N = 4\ell^3$ atoms (FIG. 1), the configurational Hamiltonian now reads

$$\begin{aligned} \mathcal{H}^{\text{conf}} &= \frac{1}{2} \sum_{h,k,l=1}^{2\ell} n_{hkl} \left(J_1 \sum_{|h-h'|+|k-k'|+|l-l'|=1} n_{h'k'l'} \right. \\ &\quad \left. + J_2 \sum_{|h-h''|+|k-k''|+|l-l''|=2} n_{h''k''l''} \right) \quad (3) \end{aligned}$$

with the cyclic boundary condition:

$$n_{h+2\ell,k,l} = n_{h,k+2\ell,l} = n_{h,k,l+2\ell} = n_{h,k,l} \quad (4)$$

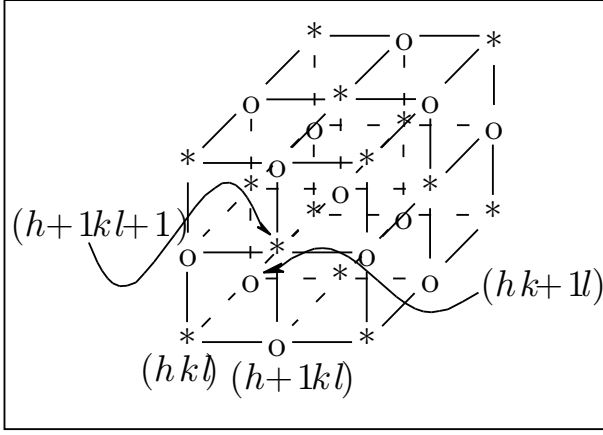


FIG. 1: The way we label the lattice sites (“*”) and interstitial sites (“o”).

that eliminates the surface and the atom number conservation condition:

$$\sum_{h,k,l=1}^{2\ell} n_{hkl} = N \quad (5)$$

that reduces the degree of independence for occupancy rate by one. Similar to the nomenclature in Paper I, we call the sites bearing the label (hkl) where $h+k+l$ is odd (*or* even), namely, “Na” (*or* “Cl”) sites, as lattice (*or* interstitial) sites, or vice versa. The lattice sites and interstitial sites interpenetrate, as they did in the one-dimensional (1D) model in Paper I.

In the 3D crystal, \mathcal{H}^{vib} is taken into consideration in the form of vibrational free energy

$$F^{\text{vib}} = 3Nk_B T \log \frac{h \langle \nu \rangle}{k_B T}, \quad (6)$$

where k_B is the Boltzmann constant, T is the absolute temperature, h is the Planck constant, $\langle \nu \rangle$ is the geometrical mean frequency of the crystal [20, 21]. It should be noticed that the formula above is valid in the Dulong-Petit limit – the temperature region where most melting processes take place and the heat capacity contributed by lattice vibration is asymptotically $3Nk_B$.

B. Symmetry of the Configurational Hamiltonian

We now study the symmetry properties of the configurational Hamiltonian under the transformation: $J_1 \mapsto -J_1$. This will shed light on the properties of the “liquid phase” derived from our model Hamiltonian as well as the interplay of J_1 and J_2 .

First, by using the transformation $\sigma_{hkl} = 2n_{hkl} - 1$ [23, 24, 25], one could map the model Hamiltonian in Eqn. (3) to the J_1 - J_2 model for magnetism [26], where $\sigma_{hkl} = \pm 1$:

$$\begin{aligned} & \mathcal{H}^{\text{conf}}(J_1, J_2, \{\sigma\}) - \frac{3N}{2}(J_1 + 2J_2) \\ &= \frac{1}{8} \sum_{h,k,l=1}^{2\ell} \sigma_{hkl} \left(J_1 \sum_{|h-h'|+|k-k'|+|l-l'|=1} \sigma_{h'k'l'} \right. \\ & \quad \left. + J_2 \sum_{|h-h''|+|k-k''|+|l-l''|=2} \sigma_{h''k''l''} \right), \end{aligned}$$

$$\sigma_{h+2\ell,k,l} = \sigma_{h,k+2\ell,l} = \sigma_{h,k,l+2\ell} = \sigma_{h,k,l}, \quad \sum_{h,k,l=1}^{2\ell} \sigma_{h,k,l} = 0. \quad (7)$$

The partition function corresponding to this configurational Hamiltonian reads: $Q^{\text{conf}}(J_1, J_2, T) = \sum_{\{\sigma\}} \exp(-\mathcal{H}^{\text{conf}}(J_1, J_2, \{\sigma\})/k_B T)$.

Second, we notice that the Hamiltonian is invariant under any transformations that swap interstitial sites and lattice sites, *i.e.* mappings such as $(hkl) \mapsto (h+1kl)$, $(hkl) \mapsto (hk+1l)$, $(hkl) \mapsto (hkl+1)$. (This is called “sublattice symmetry” [27].) It is conventional to assume [27] that there exists a temperature $T' \geq 0K$, above which the partition functions $Q^{\text{conf}}(J_1, J_2, T)$ and $Q^{\text{conf}}(-J_1, J_2, T)$ both preserve the “sublattice symmetry” of the Hamiltonian. In other words, when $T > T'$, both the (J_1, J_2) and $(-J_1, J_2)$ systems are characterized by equal amount of atoms occupying the lattice sites and interstitial sites. Since the number of atoms occupying either type of sites is $N/2$, we may infer that both partition functions (*i.e.* $Q^{\text{conf}}(J_1, J_2, T)$ and $Q^{\text{conf}}(-J_1, J_2, T)$) are dominated by terms with the configuration $\{\sigma\}$ satisfying:

$$\sum_{\substack{h,k,l=1 \\ (-1)^{h+k+l}=1}}^{2\ell} \sigma_{hkl} = \sum_{\substack{h',k',l'=1 \\ (-1)^{h'+k'+l'}=-1}}^{2\ell} \sigma_{h'k'l'} = 0. \quad (8)$$

So the transformation

$$\sigma_{hkl} \mapsto \sigma_{hkl}^* = (-1)^{h+k+l} \sigma_{hkl} \quad (9)$$

sends one dominant configuration

$$\{\sigma\} = \left\{ \sigma_{hkl}, h, k, l \in \{1, 2, \dots, 2\ell\} \left| \sum_{h,k,l=1}^{2\ell} \sigma_{hkl} = 0 \right. \right\} \quad (10)$$

to another dominant configuration

$$\{\sigma^*\} = \left\{ \sigma_{hkl}^*, h, k, l \in \{1, 2, \dots, 2\ell\} \left| \sum_{h,k,l=1}^{2\ell} \sigma_{hkl}^* = 0 \right. \right\} \quad (11)$$

in the partition function, and transforms the configurational Hamiltonian in the following way:

$$\begin{aligned} \mathcal{H}^{\text{conf}}(J_1, J_2, \sigma) &\mapsto \mathcal{H}^{\text{conf}}(J_1, J_2, \sigma^*) \\ &= \mathcal{H}^{\text{conf}}(-J_1, J_2, \sigma) + 3NJ_1, \end{aligned} \quad (12)$$

where

$$\begin{aligned} & \mathcal{H}^{\text{conf}}(J_1, J_2, \{\sigma^*\}) - \frac{3N}{2}(J_1 + 2J_2) \\ &= \frac{1}{8} \sum_{h,k,l=1}^{2\ell} \sigma_{hkl}^* \left(J_1 \sum_{|h-h'|+|k-k'|+|l-l'|=1} \sigma_{h'k'l'}^* \right. \\ & \quad \left. + J_2 \sum_{|h-h''|+|k-k''|+|l-l''|=2} \sigma_{h''k''l''}^* \right). \end{aligned} \quad (13)$$

From the obvious identity:

$$\sum_{\{\sigma\}} e^{-\frac{\mathcal{H}^{\text{conf}}(J_1, J_2, \{\sigma\})}{k_B T}} = \sum_{\{\sigma^*\}} e^{-\frac{\mathcal{H}^{\text{conf}}(J_1, J_2, \{\sigma^*\})}{k_B T}}, \quad (14)$$

we see that when $T > T'$, the configurational free energy ($F^{\text{conf}} \equiv -k_B T \log Q^{\text{conf}}$) has the following correspondence due to “sublattice symmetry”:

$$\begin{aligned} & F^{\text{conf}}(J_1, J_2, T) - \frac{3N}{2}(J_1 + 2J_2) \\ &= F^{\text{conf}}(-J_1, J_2, T) - \frac{3N}{2}(-J_1 + 2J_2). \end{aligned} \quad (15)$$

This equation is parallel to Eqn. (12) in Paper I, which is a formula invariant under the transformation $J_1 \mapsto -J_1$.

The analysis above reveals that when $T > T'$, the free energy of the system (up to a ground energy term that reads $(3N/2)(\pm J_1 + 2J_2)$) is sensitive to J_2 but probably insensitive to J_1 – it is because $F^{\text{conf}}(\pm J_1, J_2, T) - (3N/2)(\pm J_1 + 2J_2)$ remains unchanged even when J_1 alters its sign, manifesting the irrelevance of J_1 in this temperature region. This scenario is consistent with the previous description of the liquid phase in the “lattice

gas model” [25], that is, the properties of the system is predominantly defined by the NNN attractive bonding energy, and it is unnecessary to take the repulsion at NN distance into account.

Therefore, we have obtained the “liquid phase” solution to our model, which highlights the importance of J_2 at high temperature. In the following section, we will show that for low temperatures $T \ll T'$, our model behaves differently as compared to the conclusions above, where different J_1 parameter could change the properties of $F^{\text{conf}}(J_1, J_2, T) - 3NJ_1/2$ drastically, indicating the loss of sublattice symmetry of the free energy. We will show that at low temperatures, the energy relationship $J_1 > J_2 < 0$ binds atoms together in the solid by breaking the “sublattice symmetry”; near the melting point, the same energy relationship helps to propagate instability in the system and undermines the long-range order by revoking the “sublattice symmetry”.

III. THE VARIATIONAL APPROACH TO THE 3D FCC CRYSTAL

A. Phenomenological Parameter Expansion of the Free Energy Functional and the Model of Melting

In our probe into the 3D fcc elemental crystal, we aim to obtain a solution based on modified MFA. We first define a random variable called the local order parameter

$$L(\mathbf{r}) = (-1)^{h+k+l} \sigma_{hkl} = (-1)^{h+k+l} (2n_{hkl} - 1) \quad (16)$$

where site \mathbf{r} bears the integer label (hkl) . According to the Landau-Ginzburg theory of MFA [28], the free energy functional contributed by configurational Hamiltonian of the 3D fcc model $\mathcal{H}^{\text{conf}}$ could be expanded phenomenologically as

$$F^{\text{conf}}[L(\mathbf{r})] = -TS^{\text{conf}}[L(\mathbf{r})] + \frac{1}{2} \left(\frac{\sqrt{2}}{a} \right)^3 \int d^3\mathbf{r} \left\{ \left[(1 - L^2(\mathbf{r})) \mathcal{H}_1 + (1 - L^2(\mathbf{r}))^2 \mathcal{H}_2 \right] + \gamma [\nabla L(\mathbf{r})]^2 \right\} \quad (17)$$

where $(\sqrt{2}/a)^3 \int d^3\mathbf{r} \equiv \sum_{\mathbf{r}}$ denotes the summation over all the $2N$ sites. (Recall that the NN distance in the $2N$ sites is $a/\sqrt{2}$, so the volume of the smallest cube on the lattice is $(a/\sqrt{2})^3$, which forms the ratio between the site summation $\sum_{\mathbf{r}}$ and the spatial integration $\int d^3\mathbf{r}$.) \mathcal{H}_1 (> 0) and \mathcal{H}_2 (< 0) are two energy parameters to be determined later as functions of J_1 and J_2 . γ (> 0) is the phenomenological “domain wall energy” coefficient. The configurational entropy $S^{\text{conf}}[L(\mathbf{r})]$, which appears in the equation above, reads as the entropy of mixing [21, 24]:

$$S^{\text{conf}}[L(\mathbf{r})] = -k_B \left(\frac{\sqrt{2}}{a} \right)^3 \int d^3\mathbf{r} \left[\frac{1 - L(\mathbf{r})}{2} \log \frac{1 - L(\mathbf{r})}{2} + \frac{1 + L(\mathbf{r})}{2} \log \frac{1 + L(\mathbf{r})}{2} \right]. \quad (18)$$

$F^{\text{vib}}[L(\mathbf{r})]$ is contributed by vibrations with geometric mean frequencies $\langle \nu_l \rangle$ (lattice mode) and $\langle \nu_i \rangle$ (interstitial mode) [20], which reads

$$F^{\text{vib}}[L(\mathbf{r})] = \frac{3k_B T}{2} \left(\frac{\sqrt{2}}{a} \right)^3 \int d^3\mathbf{r} \frac{(1 - L^2(\mathbf{r}))}{4} \log \frac{\langle \nu_i \rangle}{\langle \nu_l \rangle} + \text{const} \quad (19)$$

when expanded in power series of $(1 - L^2(\mathbf{r}))$.

Now the total phenomenological free energy functional $F[L(\mathbf{r})]$ reads:

$$F[L(\mathbf{r})] = F^{\text{conf}}[L(\mathbf{r})] + F^{\text{vib}}[L(\mathbf{r})] = \left(\frac{\sqrt{2}}{a}\right)^3 \int d^3\mathbf{r} f(L(\mathbf{r}), \nabla L(\mathbf{r})) \quad (20)$$

where

$$f(L(\mathbf{r}), \nabla L(\mathbf{r})) = \left\{ \frac{1}{2} \left[(1 - L^2(\mathbf{r})) \mathcal{H}_1 + (1 - L^2(\mathbf{r}))^2 \mathcal{H}_2 - 3k_B T (1 - L^2(\mathbf{r})) \Upsilon \right] + k_B T \left[\frac{1 - L(\mathbf{r})}{2} \log \frac{1 - L(\mathbf{r})}{2} + \frac{1 + L(\mathbf{r})}{2} \log \frac{1 + L(\mathbf{r})}{2} \right] + \frac{\gamma}{2} [\nabla L(\mathbf{r})]^2 \right\}. \quad (21)$$

and $\Upsilon = (1/4) \log(\langle \nu_l \rangle / \langle \nu_i \rangle) > 0$ is a factor modeling the “lattice softening” effect, that is, interstitials have a lower vibration frequency than normal atoms at the lattice sites. By variational methods, we may apply the Euler-Lagrange equation

$$\frac{\partial f(L(\mathbf{r}), \nabla L(\mathbf{r}))}{\partial L(\mathbf{r})} = \nabla \frac{\partial f(L(\mathbf{r}), \nabla L(\mathbf{r}))}{\partial \nabla L(\mathbf{r})}, \quad (22)$$

to optimize the free energy functional with the boundary-free condition and obtain the equation of motion for $L(\mathbf{r})$ in the “Poisson equation” form:

$$\rho(L(\mathbf{r})) = -\gamma \nabla^2 L(\mathbf{r}), \quad (23)$$

where

$$\rho(L(\mathbf{r})) = \mathcal{H}_1 L(\mathbf{r}) - 2\mathcal{H}_2 L(\mathbf{r}) (L^2(\mathbf{r}) - 1) - 3k_B T L(\mathbf{r}) \Upsilon - k_B T \tanh^{-1} L(\mathbf{r}). \quad (24)$$

The “phenomenological electric charge density” $\rho(L(\mathbf{r}))$ immediately gives rise to a simple mathematical model of the catastrophe of the long-range order: For sufficiently low temperature T , the curve $\rho(L(\mathbf{r}))$ intersects the positive $L(\mathbf{r})$ -axis at least once (FIG. 2), so there is a homogeneous distribution $L(\mathbf{r}) \equiv \langle L \rangle_T \neq 0$ that makes $\rho(L(\mathbf{r}))$ vanish. When $T = T_m$, where T_m suffices

$$\rho(\langle L \rangle_{T_m}) = 0 \text{ and } \left. \frac{\partial \rho(L(\mathbf{r}))}{\partial L(\mathbf{r})} \right|_{L(\mathbf{r})=\langle L \rangle_{T_m}} = 0$$

simultaneously, the intersection becomes a tangent point and we have the following equations:

$$\begin{cases} 3\Upsilon + \frac{1}{1 - \langle L \rangle_{T_m}^2} = \frac{\mathcal{H}_1 - 2\mathcal{H}_2(3\langle L \rangle_{T_m}^2 - 1)}{k_B T_m} \\ \frac{1}{\langle L \rangle_{T_m}^3} \left(\frac{\langle L \rangle_{T_m}}{1 - \langle L \rangle_{T_m}^2} - \tanh^{-1} \langle L \rangle_{T_m} \right) = -\frac{4\mathcal{H}_2}{k_B T_m} \end{cases}, \quad (25)$$

In FIG. 2, $k_B T_m = \mathcal{H}_1/2.53$. For temperatures higher than T_m , $\rho(L(\mathbf{r}))$ no longer intersects the positive $L(\mathbf{r})$ -axis, suggesting the loss of long-range order. From

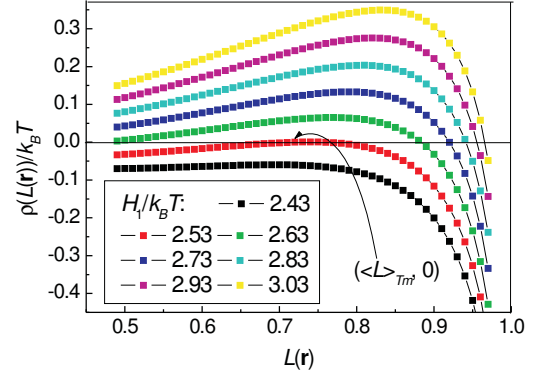


FIG. 2: (color online) Local properties of $\rho(L(\mathbf{r}))/k_B T$ near its node: $\langle L \rangle_T$. In this specific case, $\mathcal{H}_1 = 6|\mathcal{H}_2|$, $\Upsilon = \log(4/3)$. The tangent node $(\langle L \rangle_{T_m}, 0)$ is related to the melting point.

Eqn. (25) we know that as \mathcal{H}_2 tends to zero, so does $\langle L \rangle_{T_m}$. Therefore, in the absence of “virtual attraction between defects” ($\propto \mathcal{H}_2$, to be elaborated immediately in next two subsections), first-order SLPT is not possible according to this model.

B. The Cooperation Effect and the \mathcal{H}_2 Term

In the MFA scenario,

$$\begin{aligned} F[L(\mathbf{r})] &= F^{\text{vib}} - T S^{\text{conf}} + \frac{1}{2} \left(\frac{\sqrt{2}}{a}\right)^3 + \int d^3\mathbf{r} \{ (6J_1 \langle n_{\mathbf{r}} n_{\mathbf{r}'} \rangle) \\ &\quad + 12J_2 \langle n_{\mathbf{r}} n_{\mathbf{r}''} \rangle + \gamma [\nabla L(\mathbf{r})]^2 \}, \end{aligned} \quad (26)$$

where $n_{\mathbf{r}} = (\sigma_{\mathbf{r}} + 1)/2$, \mathbf{r} and \mathbf{r}' are NN sites, \mathbf{r} and \mathbf{r}'' are NNN sites. One simple-minded approximation yields the result: $\langle \sigma_{\mathbf{r}} \sigma_{\mathbf{r}'} \rangle = -\langle \sigma_{\mathbf{r}} \sigma_{\mathbf{r}''} \rangle = -L^2(\mathbf{r})$. This approximation is equivalent to the following statement:

when the correlation between sites is negligible and $L(\mathbf{r})$ distribution is uniform, the lattice (*or* interstitial) site occupancy is $(1 + |L(\mathbf{r})|)/2$ (*or* $(1 - |L(\mathbf{r})|)/2$), so that multiplication rule in probability theory infers that [24],

$$\begin{aligned} & \langle n_{\mathbf{r}} n_{\mathbf{r}'} \rangle \\ &= \frac{1 + |L(\mathbf{r})|}{2} \frac{1 - |L(\mathbf{r}')|}{2} = \frac{1 - L^2(\mathbf{r})}{4}, \end{aligned} \quad (27)$$

$$\begin{aligned} & \langle n_{\mathbf{r}} n_{\mathbf{r}''} \rangle \\ &= \frac{1}{2} (\langle n_{\mathbf{r}} n_{\mathbf{r}''} \rangle_{\text{lattice sites}} + \langle n_{\mathbf{r}} n_{\mathbf{r}''} \rangle_{\text{interstitial sites}}) \\ &= \frac{1}{2} \left[\left(\frac{1 + |L(\mathbf{r})|}{2} \right)^2 + \left(\frac{1 - |L(\mathbf{r}')|}{2} \right)^2 \right] \\ &= \frac{1}{2} - \frac{1 - L^2(\mathbf{r})}{4}. \end{aligned} \quad (28)$$

Such an argument is reasonable when $|L(\mathbf{r})|$ is sufficiently close to 1 and the interstitial concentration is low enough to obscure the cooperation between defects. When $\Upsilon = 0$, the approximation above gives the defect concentration in the form of $(1 - |L(\mathbf{r})|)/2 \sim \exp(-u/2k_B T)$ where $u = 6J_1 - 12J_2$ is the excitation energy of one interstitial

defect. This asymptotic behavior of the partition function agrees with the well-established theory of Frenkel defects where excitations of defects are assumed to be spatially independent [20].

However, the approximation $\langle \sigma_{\mathbf{r}} \sigma_{\mathbf{r}'} \rangle = -\langle \sigma_{\mathbf{r}} \sigma_{\mathbf{r}''} \rangle$ is far from accurate when the interstitial concentration is high and correlation between atoms should be taken with care. By the qualitative analysis of the exact partition function, we see from Eqn. (8) that $\langle \sigma_{\mathbf{r}} \sigma_{\mathbf{r}'} \rangle$ vanishes in MFA scenario when $T > T'$, so that $F^{\text{conf}}(J_1, J_2, T) - 3NJ_1/2$ is independent from J_1 when $T > T'$ while employing MFA. However, it does not follow that $\langle \sigma_{\mathbf{r}} \sigma_{\mathbf{r}''} \rangle = -\langle \sigma_{\mathbf{r}} \sigma_{\mathbf{r}'} \rangle = 0$. We thus have to make corrections to the estimate of $\langle \sigma_{\mathbf{r}} \sigma_{\mathbf{r}''} \rangle$, especially when $|L(\mathbf{r})|$ is far away from 1. To see the indispensability of this correction, we re-examine the partition function from the graph-theoretic perspective. In the thermodynamic limit, when $T > T'$, by replacing the summation over all states with the summation over thermodynamically most probable states (which is a “steepest-descent argument” similar to Eqn. (6) in Paper I), we may write the exact partition function as:

$$\begin{aligned} Q^{\text{conf}}(J_1, J_2, T) &= \sum_{\{\sigma\}} \exp \left[-\frac{\mathcal{H}^{\text{conf}}(J_1, J_2, \sigma)}{k_B T} \right] \rightarrow \sum_{\{\sigma_{hkl}=\pm 1\}} \exp \left[-\frac{\mathcal{H}^{\text{conf}}(J_1, J_2, \sigma)}{k_B T} \right] \\ &= \frac{2^{2N} \exp \left[-\frac{3N}{2k_B T} (J_1 + 2J_2) \right]}{\cosh^{2N} \frac{J_1}{4k_B T} \cosh^{2N} \frac{J_2}{4k_B T}} \sum_{r,s} g_{r,s} \tanh^r \frac{J_1}{4k_B T} \tanh^s \frac{J_2}{4k_B T} \\ &\approx \frac{2^{2N} \exp \left[-\frac{3N}{2k_B T} (J_1 + 2J_2) \right]}{\cosh^{2N} \frac{J_2}{4k_B T}} \sum_s g_{0,s} \tanh^s \frac{J_2}{4k_B T} \end{aligned} \quad (29)$$

where $g_{r,s}$ is the number of loops that contain r antibonds (lines that join two NN sites) and s bonds (lines that join two NNN sites) and r must be an even number because every loop is closed. (The evenness of the number r confirms again the $J_1 \mapsto -J_1$ symmetry. cf. Appendix A in Paper I) The final “ \approx ” in the equation above results from the fact that $\tanh(J_1/4k_B T) \approx 0$, and that $\cosh(J_1/4k_B T) \approx 1$ since the temperature T is high enough. It follows that

$$\begin{aligned} & F^{\text{conf}}(J_1, J_2, T) - \frac{3N}{2} (J_1 + 2J_2) \\ &= -k_B T \log Q^{\text{conf}}(J_1, J_2, T) - \frac{3N}{2} (J_1 + 2J_2) \\ &= 2Nk_B T \log \cosh \frac{J_2}{4k_B T} - 2Nk_B T \log 2 - k_B T \log \left(\sum_s g_{0,s} \tanh^s \frac{J_2}{4k_B T} \right) \end{aligned} \quad (30)$$

still varies with respect to T when $T > T'$, and this variation is dependent on the NNN attractive interaction J_2 , reinforcing that $\langle \sigma_{\mathbf{r}} \sigma_{\mathbf{r}''} \rangle$ is still non-zero when $T > T'$.

From the behavior of the exact partition function, we see that the mean NNN correlation is more persistent than its NN counterpart. In other words, the system

tends to “preserve” more bonds than assumed in the approximation $\langle \sigma_{\mathbf{r}} \sigma_{\mathbf{r}'} \rangle = -\langle \sigma_{\mathbf{r}} \sigma_{\mathbf{r}''} \rangle$. The inaccurate approximation $\langle \sigma_{\mathbf{r}} \sigma_{\mathbf{r}'} \rangle = -\langle \sigma_{\mathbf{r}} \sigma_{\mathbf{r}''} \rangle$ infers that when interstitials are excited, the creation of 6 antibonds is accompanied by annihilation of exactly 12 bonds, which is not necessarily the case.

In order to offset the overestimate in the bond annihilation, we have to write down

$$6J_1 \langle n_{\mathbf{r}} n_{\mathbf{r}'} \rangle + 12J_2 \langle n_{\mathbf{r}} n_{\mathbf{r}''} \rangle = 6J_2 + (1 - L^2(\mathbf{r})) \mathcal{H}_1 + (1 - L^2(\mathbf{r}))^2 \mathcal{H}_2 \quad (31)$$

where $\mathcal{H}_1 = (3/2)(-2J_2 + J_1)$, and the *negative* coefficient \mathcal{H}_2 , which is proportional to J_2 , is to be determined in the next subsection.

C. The Phenomenological Parameters \mathcal{H}_2 and γ as Functions of J_1 and J_2

When the concentration of interstitials is considerable (about 3% ~ 5%), the creation of di-interstitials (excitation of two interstitial atoms at NNN distance) helps to preserve more NNN atom pairs than predicted in Eqn. (28). This cooperation effect inherent in the Hamiltonian lowers the energy cost in exciting interstitials because a di-interstitial has less formation energy than that of two interstitials at farther separate distance in our model [30]. Accordingly, we have to correct Eqn. (28) by adding a positive term proportional to $(1 - L^2(\mathbf{r}))^2$ (symmetry and analyticity of the free energy preclude terms including $L(\mathbf{r})$ or $|L(\mathbf{r})|$). One scheme to outline this correction is by estimating the percentage number of occurrence of NNN-contact holes in the lattice sites as

$$\frac{12}{2} \left(\frac{1 - |L(\mathbf{r})|}{2} \right)^2 \approx \frac{3}{8} (1 - L^2(\mathbf{r}))^2 \quad (32)$$

where “12” is the coordination number of NNN pairs. FIG. 3 shows how “virtual attraction” [9] between defects is taken into consideration based on probabilistic arguments. The system preserves more bonds than in the simple-minded approximation: when two holes on the lattice sites are close (in NNN contact) instead of being farther separate, they save the bond energy in the amount of J_2 . In total, the saved bonds by stochastic contact of holes lower the system energy in magnitude of $(3/8)|J_2|(1 - L^2(\mathbf{r}))^2$.

Dynamically speaking, this correction could be also understood by the NNN correlation on the lattice sites. Since the occupancy of lattice sites is approximately 1, the relaxation time of bonds on lattice sites is much longer than that of the bonds on the interstitial sites and the antibonds. So the dissociation of bonds is a “slower reaction” than the creation of antibonds. That is why $\langle n_{\mathbf{r}} n_{\mathbf{r}''} \rangle_{\text{lattice sites}}$ should be greater than $[(1 + |L(\mathbf{r})|)/2]^2$.

Therefore, after considering defect attraction or NNN correlation on the lattice sites, the ensemble average $\langle n_{\mathbf{r}} n_{\mathbf{r}''} \rangle$ should be modified into

$$\langle n_{\mathbf{r}} n_{\mathbf{r}''} \rangle = \frac{1}{2} - \frac{1 - L^2(\mathbf{r})}{4} + \frac{3}{8} (1 - L^2(\mathbf{r}))^2, \quad (33)$$

so as to account for the crystal’s tendency to retain as many NNN atom pairs (bonds) as possible. Since NN

sites are scarcely occupied by two atoms simultaneously, NN correlations are immaterial as compared to NNN correlations. In the light of this, we may retain Eqn. (27) in the final expression of free energy functional. Comparing this with Eqn. (31), we have

$$\mathcal{H}_2 = \frac{3}{8} J_2 < 0. \quad (34)$$

When spatial inhomogeneity is significant, a domain-wall energy proportional to $[\nabla L(\mathbf{r})]^2$ should be taken into account in order to offset the miscalculation (Δ) based on the “mean-field” assumption $L(\mathbf{r}) = L(\mathbf{r}') = L(\mathbf{r}'')$. In Eqn. (26), a good estimate of γ is $a^2 \mathcal{H}_1/2$ because

$$\begin{aligned} & \Delta(2J_1 \langle \sigma_{\mathbf{r}} \sigma_{\mathbf{r}'} \rangle) \\ &= 2 \left(\frac{J_1}{L(\mathbf{r}) L(\mathbf{r}')} \right) - \left(\frac{J_1}{L(\mathbf{r}) L(\mathbf{r}')} \right) - \left(\frac{J_1}{L(\mathbf{r}) L(\mathbf{r}')} \right) \\ &= -J_1 (2pr - p^2 - r^2) \\ &= J_1 (p - r)^2 = J_1 \frac{a^2}{2} [\nabla L(\mathbf{r})]^2 \end{aligned} \quad (35)$$

$$\begin{aligned} & \Delta(2J_2 \langle \sigma_{\mathbf{r}} \sigma_{\mathbf{r}''} \rangle) \\ &= 2 \left(\frac{J_2}{p L(\mathbf{r})} \right) - \left(\frac{J_2}{p L(\mathbf{r})} \right) - \left(\frac{J_2}{r L(\mathbf{r})} \right) \\ &= -J_2 a^2 [\nabla L(\mathbf{r})]^2. \end{aligned} \quad (36)$$

The total domain-wall energy contributed by the non-vanishing $\nabla L(\mathbf{r})$ at site \mathbf{r} is thus

$$\begin{aligned} & \frac{1}{4} \times 6 \times \frac{1}{2} \left(J_1 \frac{a^2}{2} - J_2 a^2 \right) [\nabla L(\mathbf{r})]^2 \\ &= \frac{a^2}{2} \mathcal{H}_1 [\nabla L(\mathbf{r})]^2. \end{aligned} \quad (37)$$

Here, the factor 1/4 results from the transformation $\sigma_{\mathbf{r}} = 2n_{\mathbf{r}} - 1$, the factor 1/2 is applied to offset repeated counting, the number 6 is a consequence of coordination number and the Pythagorean theorem applied to the $\nabla L(\mathbf{r})$ vector decomposition.

Physically speaking, at temperatures far lower than the Dulong-Petit limit, the domain wall energy could be interpreted as the energy contributed by the dislocations which destroy the continuity of $L(\mathbf{r})$ on the interface. The $(\gamma/2)[\nabla L(\mathbf{r})]^2$ term associated with rare dislocations contribute little to the total free energy at low temperatures. When temperature is sufficiently high, large fluctuations of $L(\mathbf{r})$ will be commonplace and the gradient term will become indispensable if we want to evaluate the total free energy correctly. (It should be emphasized that the vibration term containing Υ arises from *entropy* effect and does not contribute to domain wall *energy*. Even when the distribution of $L(\mathbf{r})$ is inhomogeneous, the average vibrational *energy* for every degree of freedom is the same, say, $k_B T$, regardless of vibrational frequency. Therefore, the expression of γ is not dependent on Υ .)

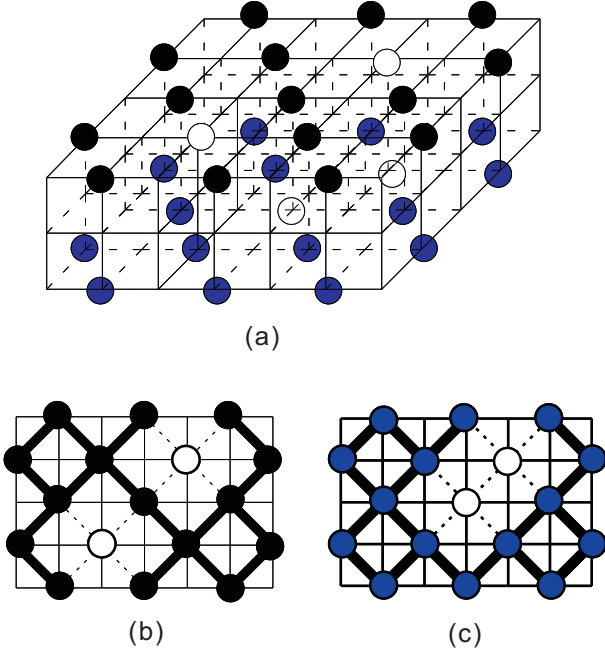


FIG. 3: (color online) (a) This shows two layers in a crystal. In the “upper layer”, two holes are separate whereas in the “lower layer”, two holes are close. (b) This shows the cross-section view of the “upper layer”, with loss of eight bonds (in dashed lines) as compared to a perfect layer. (c) This shows cross-section view of the “lower layer”, with loss of seven bonds (in dashed lines) as compared to a perfect layer. We could see that two close holes save a bonding energy in the amount of J_2 (bonds are denoted by thick black lines in (b) and (c)).

D. “Chemical Equilibrium” and its Demise Due to Locally Isotropic Instability

The physical implications behind the mathematical model outlined in Sect. III.A provide much more information about the melting pathway.

First, for $T < T_m$, we find that $\rho(\langle L \rangle_T) = 0$ is equivalent to the “chemical equilibrium” condition:

$$\frac{1 - |\langle L \rangle_T|}{1 + |\langle L \rangle_T|} = \frac{[\text{defective cell}]}{[\text{non-defective cell}]} = e^{-\frac{\Delta\bar{\epsilon}}{k_B T}}. \quad (38)$$

Here, “[.]” denotes equilibrium concentration, and

$$\Delta\bar{\epsilon} = 2(\mathcal{H}_1 - 3k_B T \Upsilon) |\langle L \rangle_T| - 4\mathcal{H}_2 |\langle L \rangle_T| (|\langle L \rangle_T|^2 - 1) \quad (39)$$

denotes the energy difference between two types of crystal cells: the *defective cell* incorporating (in the statistical parlance) more than one (inclusive) interstitial and the *non-defective cell* including less than one interstitial (inset of FIG. 4 (a)). (In Appendix A, we will derive the form of $\Delta\bar{\epsilon}$ from a perspective independent from the arguments in previous subsections.) This dynamical equilibrium is achieved by stochastic creation and annihilation of interstitials, or vividly speaking, the collisions

in a dilute “gas” of interstitial monomers and interstitial oligomers, in search of a minimal free energy corresponding to an optimized long-range order parameter $\langle L \rangle_T$ (FIG. 4 (a)).

Second, we notice that the aforementioned “collision process” causes a fluctuation of $L(\mathbf{r})$, governed by Eqn. (23) that resembles the equation for a globally neutral plasma when $T \ll T_m$. (This is because $\rho(L(\mathbf{r}))$ changes sign as $L(\mathbf{r})$ varies in the vicinity of $\langle L \rangle_T$, which is analogous to the coexistence of positive and negative charges in a plasma.) The Green function of fluctuation response $G(\mathbf{r}, \mathbf{r}')$ satisfies

$$\left(\frac{\sqrt{2}}{a}\right)^3 \left[\gamma \nabla^2 + \frac{\partial \rho(L(\mathbf{r}))}{\partial L(\mathbf{r})} \right] G(\mathbf{r}, \mathbf{r}') = -k_B T \delta(\mathbf{r} - \mathbf{r}'), \quad (40)$$

where $\delta(\mathbf{r} - \mathbf{r}')$ is the Dirac delta function (See Appendix B for the derivation of the Green function). For sufficiently low temperature $T \ll T_m$, the partial derivative in the equation above is always negative, so $G(\mathbf{r}, \mathbf{r}')$ is a propagator that decays exponentially to guarantee the stability of the homogeneous distribution $L(\mathbf{r}) \equiv \langle L \rangle_T$. However, as T approaches T_m from below, it is possible that $\partial \rho(L(\mathbf{r})) / \partial L(\mathbf{r}) > 0$ for certain values of $L(\mathbf{r})$ not far from $\langle L \rangle_T$, which results from a non-Gaussian perturbation (Appendix B) to the homogeneous distribution. In the complex wave-number plane, apart from the poles at purely imaginary wave-numbers (decay mode), the Fourier transform of the Green function would then also encounter real wave-number singularities (oscillation mode), indicating that homogeneity is only preserved for a finite volume within which fluctuation propagates as a sinusoidal wave. When $T = T_m$, which is defined in Eqn. (25), the “phenomenological electric charge density” $\rho(L(\mathbf{r}))$ no longer changes its

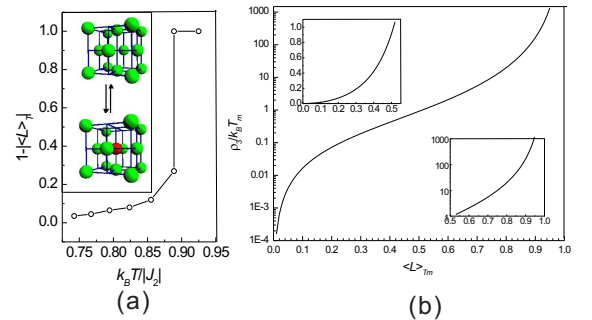


FIG. 4: (color online) (a) This plots $\langle L \rangle_T - T$ dependence for the same $\mathcal{H}_1/|\mathcal{H}_2|$ and Υ as in FIG. 2, where catastrophe occurs at the “melting point” $T_m = 0.89|J_2|/k_B$. Inset shows a “chemical equilibrium” between non-defective (up) and defective (down, interstitial defect highlighted by red) cells at $T < T_m$. (b) Plotted here is the dimensionless parameter $\rho_3/k_B T_m$ as a function of $\langle L \rangle_{T_m}$ (inset shows details of the function using different scales). ρ_3 appears in the expression of $\pi\xi$, the critical size of the liquid nucleus.

sign in the vicinity of $\langle L \rangle_{T_m}$, and could be expanded as $\rho(L(\mathbf{r})) = -\mu^2(\mathbf{r})\rho_2 - \mu^3(\mathbf{r})\rho_3 + \dots$ in the vicinity of $\langle L \rangle_{T_m}$, where $\mu(\mathbf{r}) = L(\mathbf{r}) - \langle L \rangle_{T_m}$.

Physically speaking, this expansion of $\rho(L(\mathbf{r}))$ infers that the uniform distribution $L(\mathbf{r}) \equiv \langle L \rangle_T$ is unstable when there is a radial symmetric perturbation (Y_{00} wave) of $L(\mathbf{r})$ judging the Gauss' theorem:

$$\begin{aligned} & \gamma \oint_{S=\partial V} \nabla L(\mathbf{r}) \cdot d\mathbf{S} \\ &= - \int_V \rho(L(\mathbf{r})) dV \begin{cases} > 0, & L(\mathbf{r}) > 0 \\ < 0, & L(\mathbf{r}) < 0 \end{cases} \end{aligned} \quad (41)$$

When a perturbative Y_{00} wave initiates, the surface integral boosts when the spherical volume is increased, so the value of $L(\mathbf{r})$ grows monotonously along the radial direction. Anisotropic Y_{lm} modes do not apparently lead to steady growth of $L(\mathbf{r})$ values and the related propagation of instability. It is because for Y_{lm} modes where $l > 0$, there is no such a causal relationship between the surface integral's growth and the growth of the $L(\mathbf{r})$ in the radial direction.

It can be verified mathematically that anisotropic Y_{lm} modes are quenched as $\sim r^l$ in the short range and do not account for the instability. This is because $\mu(\mathbf{r})$ satisfies:

$$\gamma \nabla^2 \mu(\mathbf{r}) = \mu^2(\mathbf{r})\rho_2 + \mu^3(\mathbf{r})\rho_3. \quad (42)$$

For anisotropic excitations, where the asymptotic behavior is $\mu(\mathbf{r}) \sim \mu(r)Y_{lm}(\theta, \phi)$, $r = |\mathbf{r}| \rightarrow 0$ (the original point of \mathbf{r} is placed at the center of excitation), $l > 0$, we find

$$\begin{aligned} \gamma \chi''(r) &= \frac{l(l+1)\gamma\chi(r)}{r^2} + \frac{\rho_2\chi^2(r)Y_{lm}(\theta, \phi)}{r} \\ &\quad + \frac{\rho_3\chi^3(r)Y_{lm}^2(\theta, \phi)}{r^2} \\ &\sim \frac{l(l+1)\gamma\chi(r)}{r^2}, \end{aligned} \quad (43)$$

where $\chi(\mathbf{r}) = |\mathbf{r}|\mu(\mathbf{r})$.

$$\mu(\mathbf{r}) \sim r^l \rightarrow 0, \text{ as } r \rightarrow 0 \quad (44)$$

Meanwhile, Y_{00} wave has the following asymptotic behavior:

$$\mu(\mathbf{r}) \sim -\frac{\rho_2}{\rho_3} \neq 0, \text{ as } r \rightarrow 0 \quad (45)$$

Therefore, isotropic excitation dominates the instability mechanism at T_m , because all the Y_{lm} ($l > 0$) modes are overwhelmed by the Y_{00} mode in the short range.

E. Relations with Born and Lindemann Criteria: "Lindemann Particle Clusters" Revisited

In the context of instability induced by locally isotropic excitations, "quasi-neutrality" in the "plasma" is attained by establishing $L(\mathbf{r}) > 0$ and $L(\mathbf{r}) < 0$ domains,

each in diameter of $\pi\xi \sim \sqrt{2}a\mathcal{H}_1^2\pi^3(2\rho_3k_BT_m)^{-1}$ (Appendix B elaborates on this estimate, and FIG. 4(b) plots the dimensionless parameter ρ_3/k_BT_m), which is the average size of the locally isotropic excitations of atom clusters. These highly cooperative and energetic atom clusters gives rise to a catastrophe of global long-range order at T_m :

$$|\langle L \rangle_T| \begin{cases} \rightarrow |\langle L \rangle_{T_m}| \neq 0, & T \rightarrow T_m - 0 \\ = 0, & T > T_m \end{cases} \quad (46)$$

The vanishing long-range order $|\langle L \rangle_T|$ at temperatures higher than T_m casts the system into sublattice symmetry.

Such locally isotropic excitations near T_m form spherical domains of instability (SDIs) and amount to one possible interpretation for the origin of "Lindemann particles" [5] and their aggregation. In such SDIs, due to the nature of the fluctuation and the relaxation, the displaced atoms are moving collaboratively, energetically and isotropically, so that we could regard them as the physical entity that bridges Born and Lindemann criteria at the melting point according to the following argument: On one hand, the totality of atoms in each SDI exhibits isotropy, which guarantees exactly vanishing shear moduli difference: $\Delta C_S = 0$ – that is, SDIs satisfy Born criterion; On the other hand, the displacement of the atoms in all the SDIs exceeds $a\delta_L^*$ – that is, the average displacement of all atoms in the Euclidean space, which packed spheres cannot perfectly fill. In the light of this, the atoms in SDIs are "Lindemann particles" by definition – that is, SDIs also satisfy Lindemann criterion.

In short, the locally isotropic plasma instability at the superheating limit ("melting point" of a surface-free solid) T_m is initiated and propagated by SDIs, and T_m is exactly the temperature at which Born and Lindemann criteria coincide. These SDIs declare the demise of the chemical equilibrium originally established by collisions in a dilute "gas" of interstitial defects, and undermine the long-range order in a solid in the mean time.

IV. DISCUSSIONS

From the arguments in the last section, we have provided accounts for the instability mechanism (*why*), molecular pathway (*how*) and phase transition temperature (*when*) related to the melting of a surface free fcc elemental crystal. The answers to *why* and *how* also help to clarify the physical basis for the equivalence of Born and Lindemann criteria. This section will provide further implications of our theoretical model and give answers to the numbered questions in the Introduction.

The crucial instability mechanism (*why*) of melting is found to be the cooperative creation of interstitials that caused the avalanche of displaced atoms. The cooperation effect transfers the information of one displaced atom isotropically to its neighborhood and finally results in the formation of SDIs. The residual shear modulus at the

melting point is due to the inability of spherical domains to fully occupy the Euclidean space. Born's argument is still valid within each SDI, but no longer valid in the melting crystal as a whole. This answers Question 1.

Therefore, for the whole crystal, lattice softening or vanishing shear modulus is not as decisive in the melting process as the cooperation effect is. In the melting point formula Eqn. (25), it is clear that the first order transition disappears when \mathcal{H}_2 is zero. The cooperation between the interstitials proves to lower the energy cost to excite defects thereby paving the way for destroying the long range order in the lattice. For fixed bonding energy J_2 and lattice softening Υ , T_m is lowered when $|\mathcal{H}_2|/|\mathcal{H}_1|$

ratio is enhanced, which is in accordance with the 1D exact solution which relates high $|J_2|/|J_1|$ ratio to great disorder.

To justify this, we will prove the following

Theorem:

$$\left(\frac{\partial T_m}{\partial \mathcal{H}_1}\right)_{\mathcal{H}_2, \Upsilon} > 0 \quad (47)$$

in the 3D fcc case.

Proof: From Eqn. (25), pick $\langle L \rangle_{T_m} > 0$, we may arrive at the following conclusion:

$$\frac{\partial}{\partial \langle L \rangle_{T_m}} \left(\frac{\mathcal{H}_1 - 3k_B T \Upsilon}{|\mathcal{H}_2|} \right) = - \frac{4 \langle L \rangle_{T_m} \left(1 - \langle L \rangle_{T_m}^2 \right)^2 \tanh^{-1} \langle L \rangle_{T_m}}{\left[\langle L \rangle_{T_m} - \left(1 - \langle L \rangle_{T_m}^2 \right) \tanh^{-1} \langle L \rangle_{T_m} \right]^2} \int_0^{\langle L \rangle_{T_m}} \frac{8x^4 dx}{(1-x^2)^3} < 0. \quad (48)$$

Therefore, we have the following argument:

$$\left. \begin{array}{l} |\mathcal{H}_2| \text{ is fixed} \\ T_m \nearrow \end{array} \right\} \xRightarrow{\text{Eqn. (25)}} \langle L \rangle_{T_m} \searrow \implies \left. \begin{array}{l} \mathcal{H}_1 - 3k_B T \Upsilon \nearrow \\ |\Upsilon| \text{ is fixed, } T_m \nearrow \end{array} \right\} \implies \mathcal{H}_1 \nearrow.$$

Thus, $(\partial T_m / \partial \mathcal{H}_1)_{\mathcal{H}_2, \Upsilon} > 0$ is evident. ■

That is to say, T_m is not only determined by the bonding energy related to \mathcal{H}_2 , but is also modulated by the difficulty to create interstitials, which is signified by \mathcal{H}_1 – the energy barrier that hinders information transfer between atoms. The mathematical inequality above could be physically interpreted as “the better information transfer, the lower melting point”. Unlike the liquid-gas phase transition involving the thorough dissociation of bonding atom pairs, in which J_2 plays a decisive rôle in determining the boiling point, the SLPT is possible when destruction of the lattice structure and the excitation of interstitials are both highly encouraged. Therefore, some materials could have high boiling points and “disproportionately” low melting points, if they have a large $|\mathcal{H}_2|$ and a small $|\mathcal{H}_1|$. (This may have shed light on the peculiar behavior of Ga and In, two metals that melt near room temperature and boil at thousands of Kelvins, although neither metal falls into the category of fcc structure.) The lattice softening $\Upsilon > 0$ is also conducive to melting in that $\mathcal{H}_1 - 3k_B T \Upsilon < \mathcal{H}_1$ enhances the apparent $|\mathcal{H}_2|/|\mathcal{H}_1|$ ratio. From this we know that the atom displacement and lattice softening are mutually complementary and this rule underlies the intrinsic relation between Lindemann and Born criteria.

The atom-scale pathway (*how*) of melting is spatial correlations of atom occupancy fluctuations. The correlation-response scheme proves to be the effective

way to transfer information in the 3D system discussed in this paper. The anomalous sinusoidal correlation wave results from the non-Gaussian fluctuations of atoms. In Ref. [5], it was observed that melting is preceded by the non-Gaussian behavior of atom displacement, but the causal relationship between the deviation from normal distribution and the SLPT was not explicitly established. This paper presents a clear demonstration of this causality in Sect. III.D and E. From the conclusions in those subsections, we may find the critical diameter of the SDIs for the example shown in FIG. 3 (b): $\pi \xi_{\min} = 15.03a$, and the spherical volume $\pi(\pi \xi_{\min})^3/6 = 1780a^3$ which contains 890 atoms in average. This forms a good comparison with the statement in Ref. [5] that the “Lindemann particle” clusters consist of $10^2 - 10^3$ atoms. The critical volume of the liquid nucleus $\pi(\pi \xi_{\min})^3/6$ will be evaluated in detail in Appendix B.

By exploring the atom-scale pathway in the thermodynamic limit, we highlight the fluctuations that propagate as a sinusoidal wave. This wave cuts the space into separate compartments exhibiting ostentatiously mutual independence, and is thus responsible for the illusion that the inhomogeneous instability suddenly emerges from nowhere. There is no contradiction between the nucleation and the thermodynamic limit, after all. This answers Question 2.

The melting point (*when*) is defined in Eqn. (25) and it is shown to be the superheating limit predicted by Born

and Lindemann criteria simultaneously. When rewritten, the melting formula takes the form

$$T_m = \frac{3|J_2|\langle L \rangle_{T_m}^3}{2k_B \left(\frac{\langle L \rangle_{T_m}}{1 - \langle L \rangle_{T_m}^2} - \tanh^{-1} \langle L \rangle_{T_m} \right)} < \frac{9|J_2|}{4k_B}. \quad (49)$$

$$\frac{2}{3} < \frac{\frac{\langle L \rangle_{T_m}}{1 - \langle L \rangle_{T_m}^2} - \tanh^{-1} \langle L \rangle_{T_m}}{\langle L \rangle_{T_m}^3} \quad (50)$$

The inequality results from the following

Proof: Pick $\langle L \rangle_{T_m} > 0$,

$$\frac{\langle L \rangle_{T_m}}{1 - \langle L \rangle_{T_m}^2} - \tanh^{-1} \langle L \rangle_{T_m} - \frac{2}{3} \langle L \rangle_{T_m}^3 = \int_0^{\langle L \rangle_{T_m}} \frac{2x^4(2 - x^2) dx}{(1 - x^2)^2} > 0 \quad (51)$$

■

We can check the reasonability of the formula above by the following table:

		Ne	Ar	Kr	Xe	Rn	Cu	Ag	Au
T_E	/K	24.56	83.8	115.79	161.4	202	1357.6	1234.93	1337.33
T_b	/K	27.07	87.3	119.93	165.1	211.3	2840	2435	3129
ΔH_{vap}	/kJ mol ⁻¹	1.7326	6.447	9.029	12.636	16.4	300.3	250.58	334.4
ΔH_{fus}	/kJ mol ⁻¹	0.3317	1.188	1.638	2.297	2.89	13.05	11.3	12.55
ΔS_{fus}	/J mol ⁻¹ K ⁻¹	13.5	14.2	14.1	14.2	14.3	9.61	9.15	9.38
$ J_2 N_A$	/kJ mol ⁻¹	0.3441	1.273	1.778	2.489	3.215	52.23	43.65	57.83
$\frac{9 J_2 }{4k_B}$	/K	93.109	344.37	481.13	673.58	870.07	14134	11812	15649
T_m	/K	29.47	100.6	138.9	193.7	242.4	1629	1482	1604
$\frac{1}{2}(1 - \langle L \rangle_{T_m})$		0.0475	0.0440	0.0435	0.0430	0.0420	0.0180	0.0195	0.0160
ΔS_m	/J mol ⁻¹ K ⁻¹	8.35	8.53	8.56	8.57	8.63	10.0	9.93	10.2

In this table, all the elements (Ne, Ar, Kr, Xe and Rn from the 0 group; Cu, Ag and Au from the IB group) assume fcc structures in the solid phase. The first four rows were taken from the descriptions of individual elements in the online encyclopedia, <http://en.wikipedia.org/> (accessed Sept. 10, 2004). T_E is the equilibrium melting point of crystals with surfaces. T_b is the boiling point of the liquid. ΔH_{vap} is the heat of evaporation. ΔH_{fus} is the heat of fusion. The data in the other rows are obtained/estimated as follows: $\Delta S_{\text{fus}} = \Delta H_{\text{fus}}/T_E$ is the entropy change due to fusion; $T_m = 1.2T_E$ is an estimate of superheating limit based on Ref. [5]; $|J_2| = (\Delta H_{\text{vap}} + \Delta H_{\text{fus}})/6N_A$ is a rough estimate for the J_2 parameter, where N_A is the Avogadro's number; $\frac{1}{2}(1 - |\langle L \rangle_{T_m}|)$ is the critical concentration of interstitial defects that initiates melting, where $|\langle L \rangle_{T_m}|$ is calculated from $|J_2|$, T_m and Eqn. (25);

$$\begin{aligned} \Delta S_m &= S^{\text{conf}}|_{L(\mathbf{r}) \equiv 0} - S^{\text{conf}}|_{L(\mathbf{r}) \equiv |\langle L \rangle_{T_m}|} \\ &= N_A k_B \left[2 \log 2 + (1 - |\langle L \rangle_{T_m}|) \log \frac{1 - |\langle L \rangle_{T_m}|}{2} + (1 + |\langle L \rangle_{T_m}|) \log \frac{1 + |\langle L \rangle_{T_m}|}{2} \right] \end{aligned} \quad (52)$$

In principle,

$$\Delta S_{\text{fus}} = S^{\text{conf}}|_{L(\mathbf{r}) \equiv 0} - S^{\text{conf}}|_{L(\mathbf{r}) \equiv |\langle L \rangle_{T_E}|} + N_A k_B \log \frac{V^l}{V^s}, \quad (53)$$

where V^l and V^s are the molar volume of liquid and solid, respectively. Therefore, the disagreement between ΔS_{fus} and ΔS_m may be explained as the volume change and the T_m/T_E ratio that are not fairly covered in the

above calculation of ΔS_m . In general, the table justifies the inequality $T_m < 9|J_2|/4k_B$, and shows similar ΔS_{fus} (or ΔS_m) values for the elements in the same group. The data also suggest that melting is triggered when the

concentration of interstitial defects is very low but still high enough [31] to induce correlation and cooperation.

For noble gases Ne, Ar, Kr, Xe, Rn, the interaction mode is the well-known van der Waals force and is described by the Lennard-Jones function [5], so they share theoretically the same (and practically similar) dimensionless parameters $|\mathcal{H}_2|/|\mathcal{H}_1|$, Υ and V^l/V^s in our model. Hence they should have the same dimensionless values: $|\langle L \rangle_{T_m}|$, $|J_2|/k_B T_m$ and $\Delta S_m/N_A k_B$. Another dimensionless parameter δ_L^* could be obtained by using the following

Theorem:

$$3k_B T_m = 4\pi^2 \langle \nu^2 \rangle m (a\delta_L^*)^2 \quad (54)$$

where $\langle \nu^2 \rangle$ is the average frequency [3].

Proof: By multiplying the Newtonian equation $m\ddot{\mathbf{r}}(t) = \mathbf{F}(t)$ with $\mathbf{r}(t)$ and taking time average, we can establish the following Langevin equation

$$m\overline{\mathbf{r}(t) \cdot \ddot{\mathbf{r}}(t)} = \overline{\mathbf{r}(t) \cdot \mathbf{F}(t)}, \quad (55)$$

where m is the mass of the atom, on which a force $\mathbf{F}(t)$ is exerted at time t .

$$\begin{aligned} \overline{\mathbf{r}(t) \cdot \ddot{\mathbf{r}}(t)} &= \lim_{\tau \rightarrow \infty} \frac{1}{\tau} \int_0^\tau \mathbf{r}(t) \cdot \ddot{\mathbf{r}}(t) dt \\ &= \lim_{\tau \rightarrow \infty} \frac{1}{\tau} \int_0^\tau \mathbf{r}(t) \cdot d\dot{\mathbf{r}}(t) \\ &= \lim_{\tau \rightarrow \infty} \frac{1}{\tau} [\mathbf{r}(t) \cdot \dot{\mathbf{r}}(t)|_{t=0}^\tau] - \lim_{\tau \rightarrow \infty} \frac{1}{\tau} \int_0^\tau \dot{\mathbf{r}}^2(t) dt \end{aligned} \quad (56)$$

$\mathbf{r}(t) \cdot \dot{\mathbf{r}}(t)|_{t=0}^\tau$ is finite insofar as vibration and Brownian motion are concerned. So $\lim_{\tau \rightarrow \infty} (1/\tau) \mathbf{r}(t) \cdot \dot{\mathbf{r}}(t)|_{t=0}^\tau = 0$, and $\overline{\mathbf{r}(t) \cdot \ddot{\mathbf{r}}(t)} = -\overline{\dot{\mathbf{r}}^2(t)}$. According to the ergodicity argument, we may replace the time average by the ensemble average as long as $T < T_m$. Therefore,

$$\begin{aligned} \overline{m\mathbf{r}(t) \cdot \ddot{\mathbf{r}}(t)} &= -m\overline{\dot{\mathbf{r}}^2(t)} = -m\langle \dot{\mathbf{r}}^2 \rangle = -3k_B T \\ \overline{\mathbf{r}(t) \cdot \mathbf{F}(t)} &= \langle \mathbf{r} \cdot \mathbf{F} \rangle = -4\pi^2 m \langle \nu^2 \mathbf{r} \cdot \mathbf{r} \rangle \end{aligned} \quad (57)$$

Define $\langle \nu^2 \rangle = \langle \nu^2 \mathbf{r}^2 \rangle / \langle \mathbf{r}^2 \rangle$ [3], then we have

$$\begin{aligned} \lim_{T \rightarrow T_m - 0} 3k_B T &= \lim_{T \rightarrow T_m - 0} 4\pi^2 m \langle \nu^2 \rangle \langle \mathbf{r}^2 \rangle \\ \parallel &\parallel \\ 3k_B T_m &= 4\pi^2 m \langle \nu^2 \rangle (a\delta_L^*)^2 \end{aligned} \quad (58)$$

■ For Lennard-Jones potential, $m \langle \nu^2 \rangle \propto |\mathcal{H}_2| \propto T_m$, so there is a universal δ_L^* for all fcc crystals governed by van der Waals forces. In our model, $k_B T_m / |J_2|$ is a function of $|\langle L \rangle_{T_m}|$ that varies slowly with respect to $|\langle L \rangle_{T_m}|$. The variation itself infers that δ_L^* is not a universal constant independent of interaction force, and the slow variation explains the reason why similar materials have nearly

identical δ_L^* 's. In a nutshell, the most influential factors for the critical Lindemann ratio δ_L^* are the profile (*not* every detail!) of the interatomic force that determines $\langle L \rangle_{T_m}$ as a function of J_1, J_2 and Υ in different crystals. There is no such a strictly universal δ_L^* for fcc lattice [7]. This answers Question 3.

We admit that the current model solution may need further refinement in terms of parameter estimate. The relations $\mathcal{H}_2 = (3/8)J_2$, $\gamma = a^2 \mathcal{H}_1 / 2$ and the representation of $\pi \xi_{\min}$ in this work are obtained by bold assumptions and simplifications. However, judging the physical origin of the collaborative effect and domain wall energy, it is clear that $\mathcal{H}_2 < 0$, $\gamma > 0$ is not questionable even when they are evaluated exactly. $\rho_3 > 0$ is also guaranteed in all cases:

Theorem: $\rho_3 > 0$ at $T = T_m$

Proof:

$$\begin{aligned} 6\rho_3 &= \frac{\partial^3}{\partial^3 \lambda} (2\mathcal{H}_2 \lambda^3 + k_B T_m \tanh^{-1} \lambda) \\ &= 12\mathcal{H}_2 + 2k_B T_m \frac{4\lambda^2 + (1 - \lambda^2)}{(1 - \lambda^2)^3} \\ &= k_B T_m \left[-\frac{3}{\lambda^3} \left(\frac{\lambda}{1 - \lambda^2} - \tanh^{-1} \lambda \right) + 2 \frac{3\lambda^2 + 1}{(1 - \lambda^2)^3} \right] \\ &= \frac{48k_B T_m}{\lambda^3} \int_0^\lambda \frac{x^4 dx}{(1 - x^2)^4} > 0, \end{aligned} \quad (59)$$

where $\lambda = \langle L \rangle_{T_m}$. ■

This immediately justifies the representation of $\pi \xi \sim \sqrt{2a\mathcal{H}_1^2 (2\rho_3 k_B T_m)^{-1}} > 0$. Both the diagram in FIG. 4(b) and analytical expression here show that

$$\lim_{\langle L \rangle_{T_m} \rightarrow 0} \frac{\rho_3}{k_B T_m} = 0. \quad (60)$$

Hence,

$$\lim_{\langle L \rangle_{T_m} \rightarrow 0} \pi \xi = \infty. \quad (61)$$

This reminds us of the infinite correlation length that characterizes the critical point of a *continuous* phase transition – now a limit case of a sequence of first-order SLPTs.

Fortunately, the effectiveness of most of the inferences in our model depends on the sign of the parameters instead of their exact values, so the related physical picture of melting will not change even if parameter estimates are modified by better methods.

V. CONCLUSIONS

In Paper II, we have provided the detailed arguments involved in the SLPT model for a 3D fcc elemental crystal. We have used two independent approaches to obtain the same equation for the evolution of defect concentration. The solution of the model shows that the phenomenological concerns in Lindemann and Born criteria:

atom displacement and lattice softening alone are only conducive to, but not decisive in the melting process. The two criteria bespeak the underlying cooperative creation of interstitials and inter-defect correlations, which are crucial for the feasibility of a first-order SLPT marked by catastrophes of both rigidity and displacement. The sinusoidal correlation waves give rise to interstitial clusters near the melting point and trigger the heterogeneous formation of the SDIs – the pre-liquid droplets satisfying Born and Lindemann criteria simultaneously.

APPENDIX A: THE DEFECT CONCENTRATION EQUATION REVISITED

1. “Chemical Equilibrium” Without \mathcal{H}_2 and Υ

In this subsection, we will provide an alternative derivation of the “chemical equilibrium” condition Eqn. (38) so as to double-check Eqn. (23). For simplicity, vibration is provisionally neglected in the following

few paragraphs.

We set out to evaluate the configurational energy difference between defective and non-defective cells when $(1 + |\langle L \rangle_T|)/2 = P$ and $(1 - |\langle L \rangle_T|)/2 = q$. Here, P is the probability that a site is occupied “correctly” and $q = 1 - P$. We use the following diagrams to aid calculation, bearing in mind that each edge in the cube below is shared by four cubes and each diagonal line on the surface of the cube is shared by two cubes. Every vertex of the cube (shared by eight cubes) is labeled by the site occupancy – the probability that the corresponding site is occupied by an atom.

If NNN correlation is negligible, we may use the following graph counting to evaluate the average energy difference between a non-defective and a defective cell:

$$-\frac{\Delta \bar{\epsilon}}{4} = \frac{1}{4} (\bar{\epsilon}_{\text{non-defective cell}} - \bar{\epsilon}_{\text{defective cell}}) \quad (\text{A1})$$

$$\begin{aligned}
 &= \left(\begin{array}{c} P \\ q \quad 1 \end{array} \begin{array}{c} P \\ q \end{array} \begin{array}{c} 0 \\ q \end{array} \right) - \left(\begin{array}{c} q \\ P \quad 1 \end{array} \begin{array}{c} q \\ P \end{array} \begin{array}{c} 0 \\ P \end{array} \right) \\
 &= \left[\begin{array}{c} P \\ q \quad 1 \end{array} \begin{array}{c} P \\ q \end{array} \begin{array}{c} 0 \\ q \end{array} \right] + \left[\begin{array}{c} P \\ q \quad 1 \end{array} \begin{array}{c} P \\ q \end{array} \begin{array}{c} 0 \\ P \end{array} \right] + \left[\begin{array}{c} P \\ q \quad 1 \end{array} \begin{array}{c} P \\ q \end{array} \begin{array}{c} 0 \\ q \end{array} \right] + \left[\begin{array}{c} P \\ q \quad 1 \end{array} \begin{array}{c} P \\ q \end{array} \begin{array}{c} 0 \\ P \end{array} \right] + \left[\begin{array}{c} P \\ q \quad 1 \end{array} \begin{array}{c} P \\ q \end{array} \begin{array}{c} 0 \\ q \end{array} \right] \\
 &\quad - \left[\begin{array}{c} q \\ P \quad 1 \end{array} \begin{array}{c} q \\ P \end{array} \begin{array}{c} 0 \\ q \end{array} \right] + \left[\begin{array}{c} q \\ P \quad 1 \end{array} \begin{array}{c} q \\ P \end{array} \begin{array}{c} 0 \\ P \end{array} \right] + \left[\begin{array}{c} q \\ P \quad 1 \end{array} \begin{array}{c} q \\ P \end{array} \begin{array}{c} 0 \\ q \end{array} \right] + \left[\begin{array}{c} q \\ P \quad 1 \end{array} \begin{array}{c} q \\ P \end{array} \begin{array}{c} 0 \\ P \end{array} \right] + \left[\begin{array}{c} q \\ P \quad 1 \end{array} \begin{array}{c} q \\ P \end{array} \begin{array}{c} 0 \\ q \end{array} \right] \\
 &= \left(3 \frac{J_1}{4} q + 3 \frac{J_2}{2} P + 6 \frac{J_1}{4} q P + 3 \frac{J_2}{2} q^2 + 3 \frac{J_2}{2} P^2 \right) \\
 &\quad - \left(3 \frac{J_1}{4} P + 3 \frac{J_2}{2} q + 6 \frac{J_1}{4} P q + 3 \frac{J_2}{2} P^2 + 3 \frac{J_2}{2} q^2 \right) \\
 &= \frac{3}{4} (-J_1 + 2J_2) (P - q) \\
 &= \frac{3}{4} (-J_1 + 2J_2) |\langle L \rangle_T|. \quad (\text{A2})
 \end{aligned}$$

This value is equal to $-(1/4)\Delta \bar{\epsilon}$ because for each cube, the state of $2 \times (1/8) = 1/4$ atoms are definite, marked by occupancy 1 and 0 respectively. Therefore, the dynamic

equilibrium between the two types of cell requires that

$$\frac{q}{P} = \frac{1 - |\langle L \rangle_T|}{1 + |\langle L \rangle_T|} = \exp \left(-\frac{2\mathcal{H}_1 |\langle L \rangle_T|}{k_B T} \right) \quad (\text{A3})$$

where $\mathcal{H}_1 = (3/2)(J_1 - 2J_2)$. This agrees with Eqs. (23) and (38) when terms associated with \mathcal{H}_2 , Υ are neglected. As $|\langle L \rangle_T| \rightarrow 1$, Eqn. (A3) implies $q \sim \exp(-u/2k_B T)$, which agrees with the well-established theory of Frenkel defects. Here, $u = 4\mathcal{H}_1$ is the excitation energy of an interstitial defect.

2. “Chemical Equilibrium” involving \mathcal{H}_2 and Υ

When $|\langle L \rangle_T|$ is sufficiently far from unity, the cooperation and correlation between NNN atoms could not be neglected. We can estimate such NNN correlation by

$$\begin{aligned} & \left[\left(\begin{array}{c} \text{Diagram 1: A cube with sites 1, q, P, 0. Site 1 is occupied by a black dot, site q by a white dot, site P by a black dot, and site 0 by a white dot.} \end{array} \right) - 3 \left(\begin{array}{c} \text{Diagram 2: A cube with sites 1, q, P, 0. Site 1 is occupied by a black dot, site q by a white dot, site P by a black dot, and site 0 by a white dot.} \end{array} \right) \right] \\ &= \left(\frac{3J_2}{2} P^3 - 3 \frac{J_2}{2} P^2 \right) - \left(\frac{3J_2}{2} q^3 - 3 \frac{J_2}{2} q^2 \right) \\ &= -\frac{3J_2}{2} (P - q) P q \\ &= \frac{3J_2}{8} |\langle L \rangle_T| (|\langle L \rangle_T|^2 - 1). \end{aligned} \quad (\text{A4})$$

Accordingly, the chemical equilibrium condition now reads:

$$\frac{1 - |\langle L \rangle_T|}{1 + |\langle L \rangle_T|} = e^{-\frac{1}{k_B T} [2\mathcal{H}_1 |\langle L \rangle_T| - 4\mathcal{H}_2 |\langle L \rangle_T| (|\langle L \rangle_T|^2 - 1)]} \quad (\text{A5})$$

where $\mathcal{H}_2 = (3/8) J_2$, in perfect agreement with Eqs. (23) and (38) leaving alone the vibration term.

The contribution from vibrations could be easily considered by the transformation $4\mathcal{H}_1 \mapsto 4\mathcal{H}_1 - 3k_B T \log(\langle \nu_l \rangle / \langle \nu_i \rangle)$ because averagely speaking, exciting one Frenkel pair changes one eigenfrequency from $\langle \nu_l \rangle$ to $\langle \nu_i \rangle$.

The chemical equilibrium between defective and non-defective cells is reached by stochastic motion of interstitials, which guarantees sufficient randomness of NN pair states (a corollary of short relaxation time of NN atom pairs) thereby supporting the former argument that holds NN correlation to be negligible. In the mean time, NNN atom pairs have considerably long relaxation time and their correlation will lead to spatial inhomogeneity, which is to be elaborated in the Appendix B.

APPENDIX B: THE SPATIAL CORRELATION OF EXCITATIONS IN DETAIL

1. The Green Function

In this subsection, we establish the equation of order correlation functions and obtain expressions for the correlation length at low temperatures. We now start to work with the unit system where $a = \sqrt{2}$. In this special system, $\int d^3 \mathbf{r}$ could be interpreted as the summation over the $2N$ sites as well as the volume integration.

postulating that the three sites that are NNN neighbor to the probability-one-occupied site tend to be occupied or be unoccupied simultaneously. Considering this cooperation effect, we should modify $-(1/4)\Delta\bar{\epsilon}$ by adding the contribution from the following diagrams:

$$\left[\left(\begin{array}{c} \text{Diagram 3: A cube with sites 1, q, P, 0. Site 1 is occupied by a white dot, site q by a black dot, site P by a white dot, and site 0 by a black dot.} \end{array} \right) - 3 \left(\begin{array}{c} \text{Diagram 4: A cube with sites 1, q, P, 0. Site 1 is occupied by a white dot, site q by a black dot, site P by a white dot, and site 0 by a black dot.} \end{array} \right) \right]$$

The equation of $L(\mathbf{r})$ spatial correlation Green function is obtained by the following procedure [27]:

(1) We introduce a phenomenological external field $H(\mathbf{r})$ and rewrite the free energy functional as

$$F[L(\mathbf{r}), H(\mathbf{r})] = F[L(\mathbf{r})] - \int d^3 \mathbf{r} H(\mathbf{r}) L(\mathbf{r}). \quad (\text{B1})$$

(2) We use functional derivative δ to verify

$$\begin{aligned} & -\frac{\delta^2 F[L(\mathbf{r}), H(\mathbf{r})]}{\delta H(\mathbf{r}) \delta H(\mathbf{r}')} \\ &= k_B T \left[\frac{1}{Q} \frac{\delta^2 Q}{\delta H(\mathbf{r}) \delta H(\mathbf{r}')} - \frac{1}{Q} \frac{\delta Q}{\delta H(\mathbf{r})} \frac{1}{Q} \frac{\delta Q}{\delta H(\mathbf{r}')} \right] \\ &= \frac{1}{k_B T} [\langle L(\mathbf{r}) L(\mathbf{r}') \rangle - \langle L(\mathbf{r}) \rangle \langle L(\mathbf{r}') \rangle] \\ &= \frac{1}{k_B T} G(\mathbf{r}, \mathbf{r}') \end{aligned} \quad (\text{B2})$$

where $Q = \exp(-F/k_B T)$.

(3) On the other hand, $\delta F[L(\mathbf{r}), H(\mathbf{r})] / \delta L(\mathbf{r}) = 0$ implies that

$$-\gamma \nabla^2 L(\mathbf{r}) - \rho(L(\mathbf{r})) - H(\mathbf{r}) = 0. \quad (\text{B3})$$

Recalling that

$$\frac{\delta \langle L(\mathbf{r}) \rangle}{\delta H(\mathbf{r}')} = -\frac{\delta^2 F[L(\mathbf{r}), H(\mathbf{r})]}{\delta H(\mathbf{r}) \delta H(\mathbf{r}')} \quad (\text{B4})$$

and

$$\frac{\delta H(\mathbf{r})}{\delta H(\mathbf{r}')} = \delta(\mathbf{r} - \mathbf{r}'), \quad (\text{B5})$$

we apply the functional differentiation to obtain:

$$\begin{aligned} 0 &= \frac{\delta}{\delta H(\mathbf{r}')} [-\gamma \nabla^2 L(\mathbf{r}) - \rho(L(\mathbf{r})) - H(\mathbf{r})] \\ &= \frac{1}{k_B T} \left[-\gamma \nabla^2 - \frac{\partial \rho(L(\mathbf{r}))}{\partial L(\mathbf{r})} \right] G(\mathbf{r}, \mathbf{r}') - \delta(\mathbf{r} - \mathbf{r}'). \end{aligned} \quad (\text{B6})$$

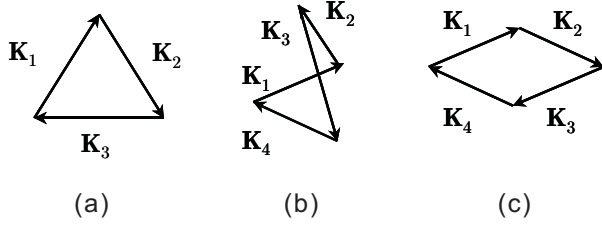


FIG. 5: (a) $\mathbf{K}_1 + \mathbf{K}_2 + \mathbf{K}_3 = 0$ where $|\mathbf{K}_1| = |\mathbf{K}_2| = |\mathbf{K}_3|$. (b) $\mathbf{K}_1 + \mathbf{K}_2 + \mathbf{K}_3 + \mathbf{K}_4 = 0$ where $|\mathbf{K}_1| = |\mathbf{K}_2| = |\mathbf{K}_3| = |\mathbf{K}_4|$. In general, such “off-plane” term $\mu(\mathbf{K}_1)\mu(\mathbf{K}_2)\mu(\mathbf{K}_3)\mu(\mathbf{K}_4)$ does not contain $|\mu(\mathbf{K}_1)|^2$ explicitly. (c) “In-plane” four wave vectors. In such case, $\mu(\mathbf{K}_1)\mu(\mathbf{K}_2)\mu(\mathbf{K}_3)\mu(\mathbf{K}_4) = |\mu(\mathbf{K}_1)|^2 |\mu(\mathbf{K}_2)|^2$.

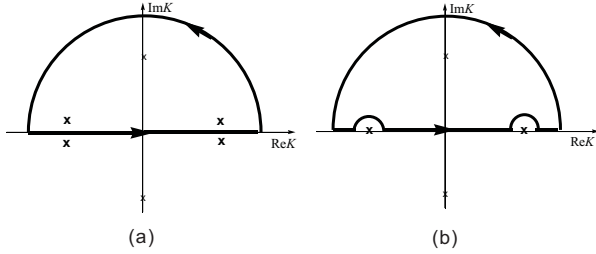


FIG. 6: (a) This plots the poles (x) and the integration contour (thick lines) for $M_\epsilon(K)$ in the complex K plane. According to Jordan’s lemma, only the residues at the poles in the upper plane are taken into account. (b) This plots the poles (x) and the integration contour (thick lines) for $M(K)$. Note that the 4 poles of $M_\epsilon(K)$ near the real axis are merged as $4/2=2$ poles in $M(K)$, so every pole on the real axis is wound around only half a circle in the contour designed for $M(K)$.

which is equivalent to Eqn. (40). It is clear that $G(\mathbf{r}, \mathbf{r}')$ is the propagator of Eqn. (23).

For $T \ll T_m$, where T_m is defined by Eqn. (25), $\rho(L(\mathbf{r}))$ is almost linear in the vicinity of $\langle L \rangle_T$, so $-\partial\rho(L(\mathbf{r}))/\partial L(\mathbf{r})$ is almost a constant ρ_1 even when fluctuation is considered. The solution of the propagator

is then

$$G(\mathbf{r}, \mathbf{r}') = \frac{k_B T}{4\pi\gamma r} e^{-r/\xi_T^*}, r = |\mathbf{r} - \mathbf{r}'|, \quad \xi_T^* = \sqrt{\frac{\gamma}{\rho_1}}. \quad (\text{B7})$$

However, for $T \rightarrow T_m - 0$, the linearity of $\rho(L(\mathbf{r}))$ in the vicinity of $\langle L \rangle_T$ is lost and the corresponding non-Gaussian fluctuations of $L(\mathbf{r})$ in different magnitudes have different propagation modes and correlation length. A fluctuation characterized by $|L(\mathbf{r})| > |\langle L \rangle_{T_m}|$ decays exponentially (because $\partial\rho(L(\mathbf{r}))/\partial L(\mathbf{r}) < 0$ in this case), but fluctuations with $|L(\mathbf{r})| < |\langle L \rangle_{T_m}|$ could be propagated in the form of a sinusoidal wave (because $\partial\rho(L(\mathbf{r}))/\partial L(\mathbf{r}) > 0$ in that case). The mean wavelength will be estimated in the next subsection.

Such fluctuation propagation is a consequence of plasma instability at T_m , and gives rise to collaborative atom clusters, the shape of which is nearly spherical, for the reason outlined in the next subsection.

2. The Correlation Functions When $T \rightarrow T_m - 0$

The mean wavelength of $L(\mathbf{r})$ fluctuation correlation could be estimated with the following steps:

Step 1: Define the Fourier expansion of $\mu(\mathbf{r})$ as

$$\mu(\mathbf{r}) = \sum_{\mathbf{K}} \mu(\mathbf{K}) e^{i\mathbf{K} \cdot \mathbf{r}} \quad (\text{B8})$$

so that the complex conjugate of $\mu(\mathbf{K})$ is $\mu(-\mathbf{K})$ and that

$$\nabla\mu(\mathbf{r}) = \sum_{\mathbf{K}} i\mathbf{K}\mu(\mathbf{K}) e^{i\mathbf{K} \cdot \mathbf{r}}. \quad (\text{B9})$$

Expand the free energy functional in the power series of $\mu(\mathbf{K})$ in a volume $V = 2N$ which contains $2N$ sites:

$$\begin{aligned} & F - F[\langle L \rangle_{T_m}] \\ &= \int d^3\mathbf{r} \left\{ \frac{1}{3} \mu^3(\mathbf{r}) \rho_2 + \frac{1}{4} \mu^4(\mathbf{r}) \rho_3 + \frac{\gamma}{2} [\nabla\mu(\mathbf{r})]^2 \right\} \\ &= \int d^3\mathbf{r} \left\{ \frac{\gamma}{2} \sum_{\mathbf{K}, \mathbf{K}'} (i\mathbf{K})(i\mathbf{K}') \mu(\mathbf{K}) \mu(\mathbf{K}') e^{i(\mathbf{K}+\mathbf{K}') \cdot \mathbf{r}} + \frac{\rho_2}{3} \sum_{\mathbf{K}_1, \mathbf{K}_2, \mathbf{K}_3} \mu(\mathbf{K}_1) \mu(\mathbf{K}_2) \mu(\mathbf{K}_3) e^{i(\mathbf{K}_1+\mathbf{K}_2+\mathbf{K}_3) \cdot \mathbf{r}} \right. \\ &\quad \left. + \frac{\rho_3}{4} \sum_{\mathbf{K}_1, \mathbf{K}_2, \mathbf{K}_3, \mathbf{K}_4} \mu(\mathbf{K}_1) \mu(\mathbf{K}_2) \mu(\mathbf{K}_3) \mu(\mathbf{K}_4) e^{i(\mathbf{K}_1+\mathbf{K}_2+\mathbf{K}_3+\mathbf{K}_4) \cdot \mathbf{r}} \right\} \\ &= V \sum_{\mathbf{K}} \frac{\gamma}{2} K^2 |\mu(\mathbf{K})|^2 + \frac{V\rho_2}{3} \sum_{\mathbf{K}_1+\mathbf{K}_2+\mathbf{K}_3=0} \mu(\mathbf{K}_1) \mu(\mathbf{K}_2) \mu(\mathbf{K}_3) + \frac{V\rho_3}{4} \sum_{\mathbf{K}_1+\mathbf{K}_2+\mathbf{K}_3+\mathbf{K}_4=0} \mu(\mathbf{K}_1) \mu(\mathbf{K}_2) \mu(\mathbf{K}_3) \mu(\mathbf{K}_4) \end{aligned} \quad (\text{B10})$$

where $K = |\mathbf{K}|$.

Step 2: Evaluate $\langle |\mu(\mathbf{K})|^2 \rangle$ by

$$\langle |\mu(\mathbf{K})|^2 \rangle = \int |\mu(\mathbf{K})|^2 e^{-\frac{F}{k_B T_m}} \prod_{\mathbf{K}} d\mu(\mathbf{K}) \bigg/ \int e^{-\frac{F}{k_B T_m}} \prod_{\mathbf{K}} d\mu(\mathbf{K}) \quad (\text{B11})$$

Based on the assumption that the fluctuation wave has a definite wave length $2\pi\xi$, we can assert that only $|\mathbf{K}| \approx 1/\xi$ terms dominate the sum in Eqn. (B10) (FIG. 5 and Ref. [32]) and carry out the summation only on equilateral polygons of \mathbf{K} . This results in

$$F - F[\langle L \rangle_{T_m}] = V \sum_{\mathbf{K}} \frac{\gamma}{2} K^2 |\mu(\mathbf{K})|^2 + O(\mu^3) + \frac{V\rho_3}{4} \sum_{|\mathbf{K}|=|\mathbf{K}'| \approx \xi^{-1}} |\mu(\mathbf{K})|^2 |\mu(\mathbf{K}')|^2 \quad (\text{B12})$$

where “off-plane” contributions of $\mu(\mathbf{K}_1)$ $\mu(\mathbf{K}_2)$ $\mu(\mathbf{K}_3)$ $\mu(\mathbf{K}_4)$ (FIG. 5 (b)) are assumed to be cancelled by phase randomness. By using the density of states in \mathbf{K} -space, one may find

$$\begin{aligned} (i) \quad \sum_{|\mathbf{K}'| \approx \xi^{-1}} |\mu(\mathbf{K}')|^2 &= \frac{V}{(2\pi)^3} \int_{\xi^{-1}-\Delta K}^{\xi^{-1}+\Delta K} |\mu(\mathbf{K}')|^2 4\pi K^2 dK \\ &\approx \frac{V}{6\pi^2} |\mu(\mathbf{K}')|^2 [(\xi^{-1} + \Delta K)^3 - (\xi^{-1} - \Delta K)^3] = \frac{Vc(c^2+3)}{3\pi^2} \frac{|\mu(\mathbf{K}')|^2}{\xi^3} \end{aligned} \quad (\text{B13})$$

when the “spectral width” reads $\Delta K = c\xi^{-1}$;

$$(ii) \quad \sum_{|\mathbf{K}|=|\mathbf{K}'| \approx \xi^{-1}} |\mu(\mathbf{K})|^2 |\mu(\mathbf{K}')|^2 \approx \frac{Vc(c^2+3)}{3\pi^2\xi^3} \sum_{|\mathbf{K}| \approx \xi^{-1}} |\mu(\mathbf{K})|^4, \quad (\text{B14})$$

which leads to the approximation:

$$\begin{aligned} &\int d\mu(\mathbf{K}) \exp \left\{ -\frac{V}{k_B T_m} \left[\frac{\gamma}{2} K^2 |\mu(\mathbf{K})|^2 + O(\mu^3) + \frac{\rho_3}{4} \frac{Vc(c^2+3)}{3\pi^2\xi^3} |\mu(\mathbf{K})|^4 \right] \right\} \\ &= \int d\mu(\mathbf{K}) \exp \left\{ -\frac{V}{k_B T_m} \left[\frac{\gamma}{2} K^2 |\mu(\mathbf{K})|^2 \right] \right\} \left[1 - \frac{V\rho_3}{4k_B T_m} \frac{Vc(c^2+3)}{3\pi^2\xi^3} |\mu(\mathbf{K})|^4 + O(\mu^6) \right] \\ &= \left(\frac{2k_B T_m}{V\gamma K^2} \right)^{1/2} - \frac{V\rho_3}{4k_B T_m} \frac{Vc(c^2+3)}{3\pi^2\xi^3} \frac{3}{4} \left(\frac{2k_B T_m}{V\gamma K^2} \right)^{5/2} + O\left(\frac{1}{K^7} \right) \end{aligned} \quad (\text{B15})$$

$$\begin{aligned} &\int d\mu(\mathbf{K}) |\mu(\mathbf{K})|^2 \exp \left\{ -\frac{V}{k_B T_m} \left[\frac{\gamma}{2} K^2 |\mu(\mathbf{K})|^2 + O(\mu^3) + \frac{\rho_3}{4} \frac{Vc(c^2+3)}{3\pi^2\xi^3} |\mu(\mathbf{K})|^4 \right] \right\} \\ &= \int d\mu(\mathbf{K}) [|\mu(\mathbf{K})|^2 + O(\mu^6)] \exp \left\{ -\frac{V}{k_B T_m} \left[\frac{\gamma}{2} K^2 |\mu(\mathbf{K})|^2 \right] \right\} \\ &= \frac{1}{2} \left(\frac{2k_B T_m}{V\gamma K^2} \right)^{3/2} \left[1 + O\left(\frac{1}{K^4} \right) \right] \end{aligned} \quad (\text{B16})$$

for short range correlations where the $K^2\mu^2$ term overwhelms the μ^4 term, and this finally leads to

$$\begin{aligned} \langle |\mu(\mathbf{K})|^2 \rangle &= \frac{1}{2} \left(\frac{2k_B T_m}{V\gamma K^2} \right)^{3/2} \left[\left(\frac{2k_B T_m}{V\gamma K^2} \right)^{1/2} - \frac{V\rho_3}{4k_B T_m} \frac{Vc(c^2+3)}{3\pi^2\xi^3} \frac{3}{4} \left(\frac{2k_B T_m}{V\gamma K^2} \right)^{5/2} + O\left(\frac{1}{K^7} \right) \right]^{-1} \\ &= \frac{1}{2} \frac{V\gamma K^2}{2k_B T_m} \left[\left(\frac{V\gamma K^2}{2k_B T_m} \right)^2 - \frac{V^2\rho_3}{16k_B T_m} \frac{c(c^2+3)}{\pi^2\xi^3} + O\left(\frac{1}{K^2} \right) \right]^{-1} \\ &= \frac{k_B T_m \gamma K^2}{V} \left[\gamma^2 K^4 - \frac{1}{4} \frac{\rho_3 k_B T_m}{\pi^2\xi^3} c(c^2+3) + O\left(\frac{1}{K^2} \right) \right]^{-1}. \end{aligned} \quad (\text{B17})$$

Let

$$M_\varepsilon(K) = \gamma K^2 \left[\gamma^2 K^4 - \frac{1}{4} \frac{\rho_3 k_B T_m}{\pi^2 \xi^3} c (c^2 + 3) + O\left(\frac{1}{K^2}\right) \right]^{-1}, \quad (\text{B18})$$

$$M(K) = \gamma K^2 \left[\gamma^2 K^4 - \frac{1}{4} \frac{\rho_3 k_B T_m}{\pi^2 \xi^3} c (c^2 + 3) \right]^{-1}. \quad (\text{B19})$$

where K is a complex variable in general. $M_\varepsilon(K)$ has six poles [33]. Three of these poles lie above the real axis, and the other three conjugate poles lie below the real axis. $M(K)$, which is an approximation of $M_\varepsilon(K)$, has four poles (FIG. (6)). Among the four, there are two poles on the real K axis corresponding to the four poles of $M_\varepsilon(K)$ that lie near the real axis. Each of the two poles should be regarded as half a pole that corresponds to the contribution from one upper-plane pole in $M_\varepsilon(K)$ when applying the residue theorem to evaluate the contour integral. Therefore, the coefficient before the summation of the residues at these two poles is πi instead of $2\pi i$ in the equation below. The two real-valued poles of $M(K)$ contribute to a sinusoidal wave. The Green function corresponding to this non-Gaussian fluctuation is then

$$\begin{aligned} G(r) &= \frac{V}{(2\pi)^3} \int d^3\mathbf{K} \langle |\mu(\mathbf{K})|^2 \rangle e^{i\mathbf{K}\cdot\mathbf{r}} \\ &= \frac{V}{(2\pi)^3} \int_0^{+\infty} K^2 dK \int_0^\pi e^{iKr \cos \theta} \sin \theta d\theta \int_0^{2\pi} d\phi \langle |\mu(\mathbf{K})|^2 \rangle \\ &= \frac{k_B T_m}{2\pi^2 r} \int_0^{+\infty} M_\varepsilon(K) K \sin Kr dK \\ &= -\frac{k_B T_m}{4\pi^2 r} \frac{\partial}{\partial r} \int_{-\infty}^{+\infty} M_\varepsilon(K) \cos Kr dK \\ &= -\frac{k_B T_m}{4\pi^2 r} \frac{\partial}{\partial r} \left[2\pi i \sum_{\text{Im}K>0} \text{res}(M_\varepsilon(K) e^{iKr}, K) \right] \\ &\approx -\frac{k_B T_m}{4\pi^2 r} \frac{\partial}{\partial r} \left[2\pi i \sum_{\text{Im}K>0} \text{res}(M(K) e^{iKr}, K) + \pi i \sum_{\text{Im}K=0} \text{res}(M(K) e^{iKr}, K) \right] \\ &= \frac{k_B T_m}{8\pi\gamma r} (e^{-K_0 r} + \cos K_0 r). \end{aligned} \quad (\text{B20})$$

Here,

$$K_0^4 = \frac{1}{\xi^4} = \frac{1}{4} \frac{\rho_3 k_B T_m}{\pi^2 \gamma^2 \xi^3} c (c^2 + 3) \quad (\text{B21})$$

which means

$$\xi = \frac{4\pi^2 \gamma^2 2^{3/2}}{\rho_3 k_B T_m c (c^2 + 3) a^3} \geq \frac{2\sqrt{2} \pi^2 \gamma^2}{\rho_3 k_B T_m a^3}$$

where the NNN atom distance a is restored. (The inequality results from the fact that $c \leq 1$ – that is, the maximum spectral width cannot exceed K_0 .)

Therefore,

$$\pi \xi_{\min} = \frac{2\sqrt{2} \pi^3 \gamma^2}{\rho_3 k_B T_m a^3} \quad (\text{B22})$$

gives an estimate of the minimal diameter of unstable clusters in the solid when $T = T_m$.

ACKNOWLEDGMENTS

This work is supported by National Natural Science Foundation of China and 973 project.

-
- [1] R. W. Cahn, Nature (London) **273**, 491 (1978); **323**, 668 (1986)
 - [2] J. G. Dash, Rev. Mod. Phys. **71**, 1737 (1999)
 - [3] F. A. Lindemann, Phys. Zeit. **11**, 609 (1910)
J. J. Gilvarry, Phys. Rev. **102**, 308 (1956)

- [4] M. Born, J. Chem. Phys. **7**, 591 (1939)
- [5] Z. H. Jin, P. Gumbsch, K. Lu and E. Ma, Phys. Rev. Lett. **87**, 055703 (2001)
- [6] J. L. Tallon, Phil. Mag. A **39**, 151 (1978)
- [7] G. Grimvall and S. Sjödin, Physica Scripta, **10**, 340

- (1974)
- [8] A. Trayanov and E. Tosatti, Phys. Rev. B, **38**, 6961 (1988); R. Ohnesorge, H. Löwen and H. Wagner, Phys. Rev. E, **50**, 4801 (1994); J. Q. Broughton and G. H. Gilmer, J. Chem. Phys. **79**, 5095 (1983); **79**, 5105 (1983)
 - [9] F. H. Stillinger and T. A. Weber, J. Chem. Phys. **81**, 5095 (1984)
 - [10] J. Cardy, J. Phys. A: Math. Gen. **29**, 1897 (1996)
 - [11] A. V. Granato, Phys. Rev. Lett. **68**, 974 (1992)
 - [12] M. I. Baskes, Phys. Rev. Lett. **83**, 2592 (1999)
 - [13] V. Halpern, J. Phys.:Condens. Matter **12**, 4303 (2000)
 - [14] N. Sandberg, B. Magyari-Köpe, and T. R. Mattsson, Phys. Rev. Lett. **89**, 065901 (2002)
 - [15] K. Nordlund and R. S. Averback, Phys. Rev. Lett. **80**, 4201 (1998)
 - [16] A. Bongiorno, L. Colombo, F. Cargnoni, C. Gatti and M. Rosati, Europhys. Lett., **50**, 608 (2000)
 - [17] S. Birner, J. P. Goss and R. Jones, P. R. Briddon, S. Öberg, *Proceedings of ENDEASD* (Stockholm 2000)
 - [18] J. I. Landman and C. G. Morgan, J. T. Schick, P. Papoulas and A. Kumar, Phys. Rev. B **55**, 15 581 (1997)
 - [19] K. W. Ingle, R. C. Perrin and H. R. Schober, J. Phys. F: Metal Phys, **11**, 1161 (1981)
 - [20] L. Salter, Proc. Roy. Soc. (London) **A233**, 418 (1956); L. Dobrzynski and J. Friedel, Surf. Science **12**, 649 (1968); G. Allan and M. Lannoo, in *Defects and Radiation Effects in Semiconductors* (ed. R. R. Hasiyuti), The Institute of Physics (Bristol and London), 1980
 - [21] L. D. Landau and E. M. Lifshitz, *Statistical Mechanics, Part I* (Butterworth-Heinemann, 1999)
 - [22] For the moment, we also neglect the thermal expansion of the solid, which we do not regard as the decisive driving force of melting. This is based on the commonsense that solid does not necessarily “expand to melt”. H₂O and Bi are two telling examples in which the liquid phase is even more dense than the solid phase. The densities of ice and water are $0.9 \times 10^3 \text{ kg m}^{-3}$ and $1 \times 10^3 \text{ kg m}^{-3}$ respectively. The density of solid bismuth is 9747 kg m^{-3} , less than that of the liquid counterpart: 10050 kg m^{-3} .
 - [23] R. K. Pathria, *Statistical Mechanics*, 2nd ed., Elsevier (Singapore) Pte Ltd, 2001
 - [24] Kerson Huang, *Introduction to Statistical Physics*, Taylor & Francis, 2001
 - [25] C. N. Yang and T. D. Lee, Phys. Rev. **87**, 404 (1957) T. D. Lee and C. N. Yang, Phys. Rev. **87**, 410 (1957).
 - [26] A. F. Barabanov and V. M. Berezovskii, Zh. Eksp. Teor. Fiz. **106**, 1156 (1994); H. Rosner, R. Hayn and J. Schulenburg, Phys. Rev. B **57**, 13660 (1998); J. Richter, A. Voigt, J. Schulenburg, N. B. Ivanov and R. Hayn, J. Magn. Magn. Mat. **177-181**, 737 (1998)
 - [27] N. Goldenfeld, *Lectures on Phase Transitions and the Renormalization Group* (Addison Wesley, 1992)
 - [28] V. L. Ginzburg, Sov. Phys. Solid State **2**, 1824 (1960)
 - [29] J. D. Jackson, *Classical Electrodynamics*, 3rd ed., Wiley Text Books, 1998
 - [30] Previous studies in interstitial clusters (*e.g.* Refs. [16, 19]) also showed that the excitation energy for a di-interstitial with the “dumbbell” configuration is less than that of two split interstitials. In other words, previous studies have shown that it costs less than twice the excitation energy of a single isolated interstitial to excite two interstitial defects that are in close contact.
 - [31] When defect concentration is $1/24 \approx 0.042$, roughly speaking, the 12 NNN sites adjacent to one atom report half an atom missing. The absence of half an atom in the next nearest neighbor site could make enough room for the transference of the energy and information between atoms. Such transference is responsible for the propagation of the fluctuation wave. Therefore, 3% \sim 5% concentration is also “high enough”.
 - [32] P. Bak, Phys. Rev. Lett. **54**, 1517 (1985)
 - [33] By the positive-definiteness of $\langle |\mu(\mathbf{K})|^2 \rangle$, it is easy to see that the function $M_\varepsilon(K)$ is greater than zero for all real K values. However, the function $M(K)$ is not positive-definite for all real K values. Nevertheless, this disadvantageous property of $M(K)$ does not affect the evaluation of the integral.